Electronic Supplementary Material (ESI) for Chemical Communications.

Mechanochemically Synthesised Dicyanamide Hybrid Organic-Inorganic Perovskites and their Melt-Quenched Glasses

Lauren N. McHugh,[a] Michael F. Thorne,[a] Ashleigh M. Chester,[a] Martin Etter,[b] Krunoslav Užarević,[c] and Thomas D. Bennett*[a]

[a] Department of Materials Science & Metallurgy, University of Cambridge, 27 Charles Babbage Road, Cambridge, UK, CB3 0FS.

[b] Deutsches Elektronen Synchrotron, FS-PETRA-D, P02.1, Notkestr. 85, 22607 Hamburg, Germany.

[c] Ruđer Bošković Institute, Zagreb, Croatia.

Supplementary Information

Table of Contents:

Methods:

[TPrA][Co(dca)$_3$] and [TPrA][Mn(dca)$_3$] mechanosynthesis. Manganese chloride (41.50 mg, 0.33 mmol) or cobalt chloride (42.80 mg, 0.33 mmol), sodium dicyanamide (89.00 mg, 1.00 mmol), tetrapropylammonium bromide (87.80 mg, 0.33 mmol) and a 2:1 solution of distilled water: ethanol (25 μL) were placed in a 10 mL stainless steel ball-mill jar with 2 x 10 mm stainless steel balls. The contents were ball-milled at 30 Hz for 30 minutes and removed to provide a slightly wet paste. The paste was found to be highly soluble in ambient temperature water, so samples were washed quickly with ice-cold distilled water to remove salt impurities while minimising product loss. The recovered product was then filtered under vacuum. The paste dried to form a very fine powder.

5x scale-up. Manganese chloride (207.60 mg, 1.65 mmol) or cobalt chloride (214.20 mg, 1.65 mmol), sodium dicyanamide (445.20 mg, 5.00 mmol), tetrapropylammonium bromide (439.3 mg, 1.65 mmol) and a 2:1 solution of distilled water: ethanol (125 μL) were placed in a 10 mL stainless steel ball-mill jar with 2 x 20 mm stainless steel balls. The contents were ball-milled at 30 Hz for 30 minutes and removed to provide a slightly wet paste. The paste was washed with ice-cold distilled water to remove salt impurities and was filtered under vacuum. The paste dried to form a very fine powder.

[TPrA][Fe(dca)$_3$] mechanosynthesis. Iron chloride tetrahydrate (65.30 mg, 0.33 mmol), sodium dicyanamide (89.00 mg, 1.00 mmol), tetrapropylammonium bromide (87.80 mg, 0.33 mmol) and a 2:1 solution of distilled water: ethanol (25 μL) were placed in a 10 mL stainless steel ball-mill jar with 2 x 10 mm stainless steel balls. The contents were ball-milled at 30 Hz for 30 minutes and removed to provide a slightly wet paste. The paste dried to form a powder.

Powder X-ray diffraction (PXRD). Finely ground samples were packed into flat plate discs and data were collected on a Bruker D8 Advance powder diffractometer, equipped with a LynxEye position-sensitive detector operating in Bragg-Brentano geometry and using Cu Kα radiation (λ = 1.5418 Å) through a 0.012 mm Ni filter. Diffraction patterns were recorded at 2θ values between 5-60°. Pawley refinements were performed using the TOPAS academic (V.6) software.[1]

***In situ* Powder X-ray diffraction.** The *in situ* PXRD experiments were performed at the Deutsches Elektronensynchrotron, Hamburg at PETRA III beamline P02.1. The beam size was *ca.* 1 x 1 mm^2 and λ = 0.20735 ± 0.00001 Å (59.79321 ± 0.00159 keV). The beamline was equipped with a Varex XRD4343CT detector and modified ball mill. Beam alignment and

calibration was performed using a Si standard in a PMMA milling jar. To avoid having two sample positions, the beam was aligned with the bottom of the PMMA jar. Data was processed by removing amorphous background contributed by PMMA.

Manganese chloride (124.50 mg 1.00 mmol) or cobalt chloride (128.40 mg, 1.00 mmol), sodium dicyanamide (267.00 mg, 3.00 mmol), tetrapropylammonium bromide (263.40 mg, 1.00 mmol) and a 2:1 solution of distilled water: ethanol (75 μL) were placed in a 10 mL poly(methyl methacrylate) (PMMA) jar with 2 x 10 mm stainless steel balls. The contents were ball-milled at 30 Hz for 30 minutes and removed to provide a slightly wet paste.

Simultaneous TGA-DSC (SDT). Simultaneous TGA-DSC was performed using a TA Instruments SDTQ600 for measurements under argon (Ar) and a TA Instruments SDTQ650 for measurements under nitrogen (N_2). Samples (*ca.* 5 mg) were heated in an alumina crucible at a heating rate of 10 ºC min^{-1} up to 1000 ºC under an Ar or N_2 atmosphere. To investigate the effect of cooling rate on recrystallisation, samples (*ca.* 15 mg) were heated in alumina crucible at a heating rate of 10 ºC min^{-1} up to either 240 or 260 ºC under an Ar atmosphere, before being cooled at either 10 ºC min^{-1} or 3 ºC min^{-1}. Data analysis was performed using the TA Instruments Universal Analysis software package.[2]

Differential scanning calorimetry (DSC). DSC measurements were performed on a Netzsch DSC 214 Polyma instrument, where powdered samples (*ca.* 5 mg) were placed into a sealed aluminium pan with a pierced lid. [TPrA][$Mn(dca)_3$] samples were initially heated to 30 ºC, before being heated to 275 ºC at a rate of 10 ºC min^{-1}. Samples were then cooled back down to 30 ºC at either 10 ºC min^{-1} or 3 ºC min^{-1}, before being heated for a second time to 275 ºC at 10 ºC min^{-1}. [TPrA][$Co(dca)_3$] samples were heated to 225 ºC, rather than 275 ºC and all measurements were conducted under Ar. Background correction scans were performed on an empty aluminium pan using the same heating and cooling cycles above. Data analysis was performed using the Netzsch Proteus® software package.[3]

Low-temperature DSC measurements were performed on a TA Instruments DSC Q2000, where powdered samples (*ca.* 5 mg) were placed into a sealed aluminium pan. [TPrA][$Mn(dca)_3$] samples were initially heated to 30 ºC, before being heated to 266 ºC at a rate of 10 ºC min^{-1}. Samples were then cooled to -60 ºC at 10 ºC min^{-1}, before being heated for a second time to 266 ºC at 10 ºC min^{-1}. [TPrA][$Co(dca)_3$] samples were heated to 225 ºC, rather than 266 ºC and all measurements were conducted under N_2. Data analysis was performed using the TA Instruments Universal Analysis software package.[2]

Bulk glass formation. Powdered samples of [TPrA][Mn(dca)$_3$] and [TPrA][Co(dca)$_3$] were heated in a tube furnace under flowing Ar to 260 ºC and 240 ºC respectively at a rate of 10 ºC min^{-1}. Heating was stopped as soon as the desired temperature was reached and the furnace was allowed to cool to below 100 ºC under flowing Ar, before cooling to room temperature overnight.

Scanning electron microscopy (SEM). SEM was performed using an FEI Nova NanoSEM operated at 8-15 kV for imaging, using backscattered electrons. Samples were prepared for SEM by securing to aluminium SEM pin stubs using carbon tape. Samples were then coated in gold, using an Emtech K550 sputter coater for 4 minutes with a current of 28 mA.

Chemical stability test. Aqueous solutions with pH 2, 5, 7, 10 and 13 were prepared and samples of crystalline and glass [TPrA][Mn(dca)$_3$] and [TPrA][Co(dca)$_3$] (*ca.* 15 mg) were suspended in *ca.* 2 mL of each solution for 7 days. PXRD was performed on samples which did not dissolve in the solutions to determine the stability of the materials to acidic, neutral and basic solutions.

CHN microanalysis. The elemental compositions of crystalline and glass samples were obtained on ground powdered samples (*ca.* 2 mg) using a CE440 Elemental Analyzer (Exeter Analytical).

Glass pellet formation. Powdered samples of crystalline [TPrA][Mn(dca)$_3$] and [TPrA][Co(dca)$_3$] were pressed into pellets using a 13 mm diameter dye held under a static pressure of 0.74 GPa for 1 minute. The resulting [TPrA][Mn(dca)$_3$] pellet was placed in an alumina crucible and was heated under flowing Ar to 260 ºC at a rate of 10 ºC min^{-1}. The furnace was switched off upon reaching 260 ºC and the pellet was allowed to cool to room temperature. The [TPrA][Co(dca)$_3$] pellet was clamped between 4 glass slides and 2 metal slides and was heated under flowing Ar to 240 ºC at a rate of 10 ºC min^{-1}. The furnace was switched off upon reaching 240 ºC and the pellet was allowed to cool to room temperature.

Gas adsorption. Porosity measurements were performed on a Micromeritics ASAP 2020 surface area and porosity analyzer. Samples (*ca.* 100 mg) were degassed by heating under vacuum at 100 °C for 12 hours, prior to analysis using carbon dioxide gas at 273 K. CO_2 gas uptakes at a relative pressure of 0.035 P/P_0 were determined using the Micromeritics MicroActive software.[4]

Contact Angle Measurements. An FTA1000 B class instrument was used to obtain contact angles between water and the surface of an a_9[TPrA][Co(dca)$_3$] pellet (13 mm diameter). Advancing contact angles of a droplet of water (approx. 10 µL) were measured over a period of 50 s and an average was taken. All analysis was performed using the FTA32 software package.[5] The mean contact angle was then determined after the removal of anomalous data points from the data set.

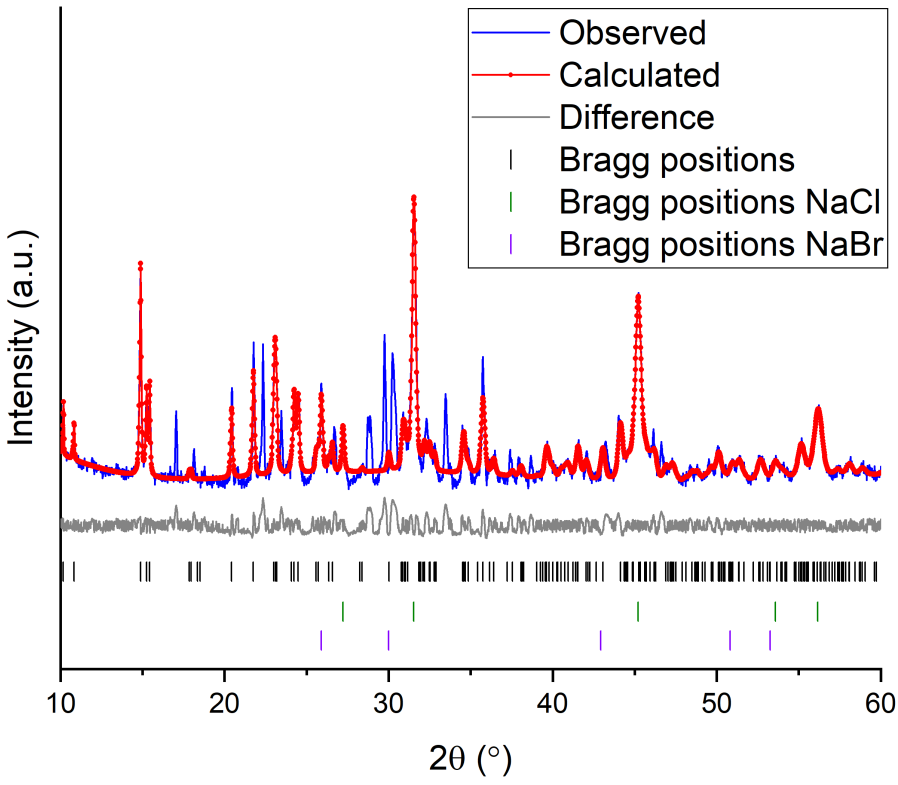

Figure S1. Pawley refinement of unwashed [TPrA][Fe(dca)$_3$]. Initial parameters were obtained from the CIF file previously reported for [TPrA][Fe(dca)$_3$].[6] NaCl and NaBr impurities were present in the sample.

R_{wp}	Space Group	Lattice Parameters	Lattice Parameters Reported for [TPrA][Fe(dca)$_3$][6]
21.703	*Ibam*	a = 11.4742(3) Å b = 11.6144(4) Å c = 17.3749(7) Å α = 90° β = 90° γ = 90°	a = 11.5219(4) Å b = 11.5355(4) Å c = 17.3841(5) Å α = 90° β = 90° γ = 90°

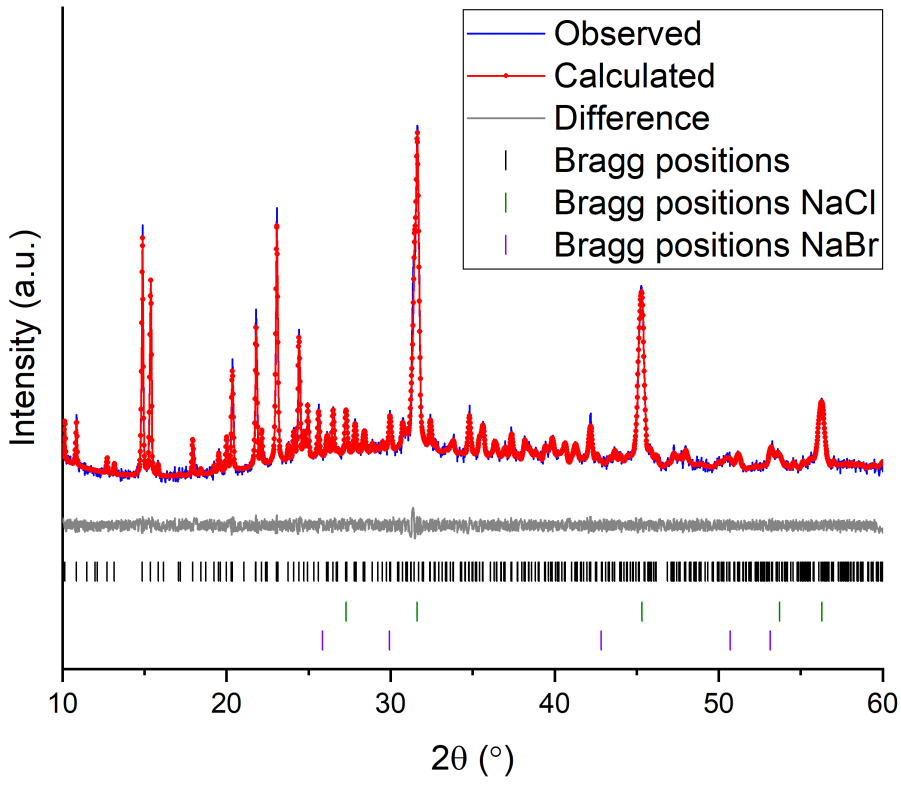

Figure S2. Pawley refinement of unwashed [TPrA][Mn(dca)$_3$]. Initial parameters were obtained from the CIF file previously reported for [TPrA][Mn(dca)$_3$].[7] NaCl and NaBr impurities were present in the sample prior to washing.

R_{wp}	Space Group	Lattice Parameters	Lattice Parameters Reported for [TPrA][Mn(dca)$_3$][7]
6.521	*P-42(1)c*	a = 16.2959(2) Å b = 16.2959(2) Å c = 17.4428(2) Å α = 90° β = 90° γ = 90°	a = 16.2752(5) Å b = 16.2752(5) Å c = 17.4231(4) Å α = 90° β = 90° γ = 90°

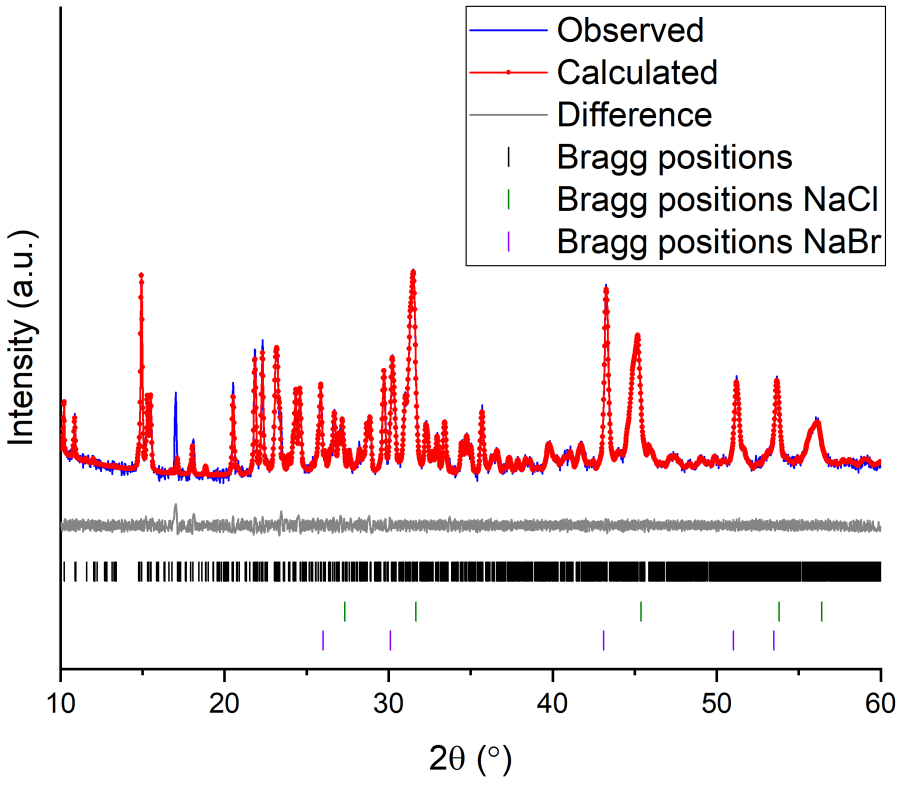

Figure S3. Pawley refinement of unwashed [TPrA][Co(dca)$_3$]. Initial parameters were obtained from the CIF file previously reported for [TPrA][Co(dca)$_3$].[6] NaCl and NaBr impurities were present in the sample prior to washing and the unidentified impurity peak at *ca.* 17º 2θ is likely unreacted starting material.

R_{wp}	Space Group	Lattice Parameters	Lattice Parameters Reported for [TPrA][Co(dca)$_3$][6]
7.702	*Pnna*	a = 17.2776(7) Å b = 23.1267(7) Å c = 22.8246(6) Å α = 90º β = 90º γ = 90º	a = 17.2246(6) Å b = 23.0205(9) Å c = 22.8310(8) Å α = 90º β = 90º γ = 90º

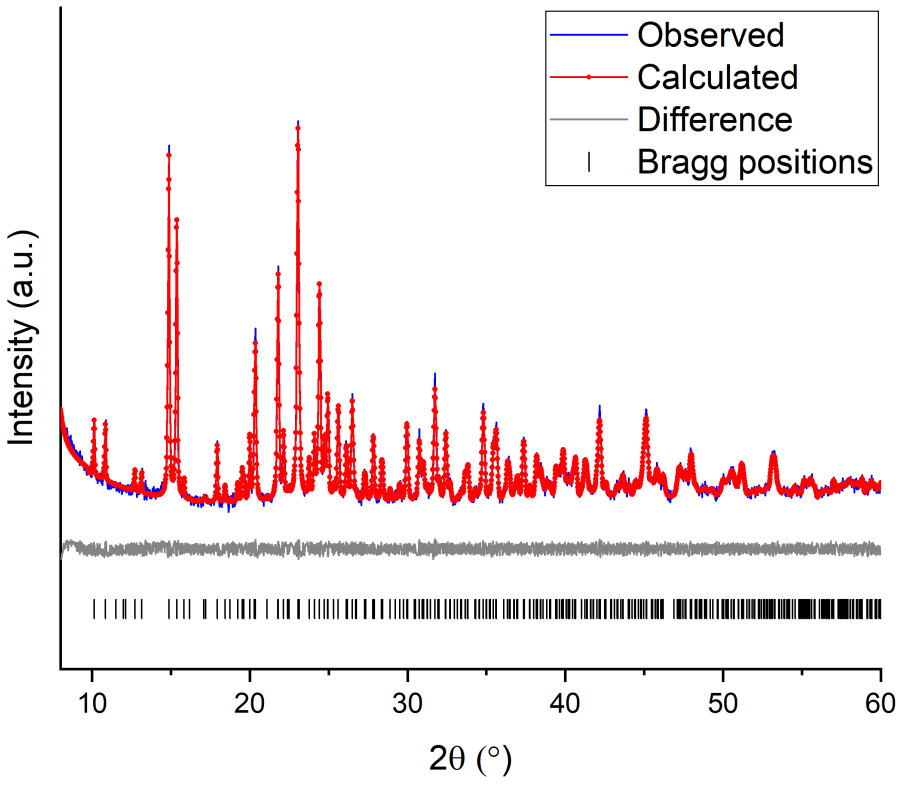

Figure S4. Pawley refinement of [TPrA][Mn(dca)$_3$]. Initial parameters were obtained from the CIF file previously reported for [TPrA][Mn(dca)$_3$].[7] The salt impurities present in the unwashed sample were removed after washing.

R_{wp}	Space Group	Lattice Parameters	Lattice Parameters Reported for [TPrA][Mn(dca)$_3$][7]
6.894	*P-42(1)c*	a = 16.2904(1) Å b = 16.2904(1) Å c = 17.4336(1) Å α = 90° β = 90° γ = 90°	a = 16.2752(5) Å b = 16.2752(5) Å c = 17.4231(4) Å α = 90° β = 90° γ = 90°

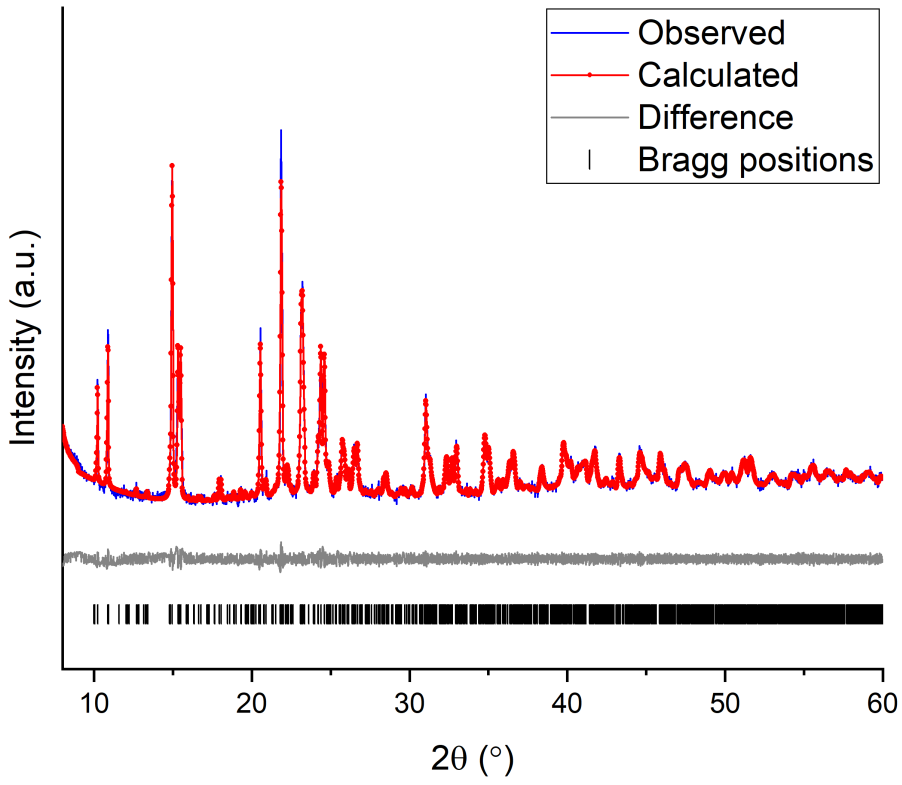

Figure S5. Pawley refinement of [TPrA][Co(dca)$_3$]. Initial parameters were obtained from the CIF file previously reported for [TPrA][Co(dca)$_3$].[6] The salt impurities and the unidentified impurity peak present in the unwashed sample were removed after washing.

R_{wp}	Space Group	Lattice Parameters	Lattice Parameters Reported for [TPrA][Mn(dca)$_3$][6]
7.067	*Pnna*	a = 17.2726(2) Å b = 23.0974(3) Å c = 22.8435(3) Å α = 90° β = 90° γ = 90°	a = 17.2246(6) Å b = 23.0205(9) Å c = 22.8310(8) Å α = 90° β = 90° γ = 90°

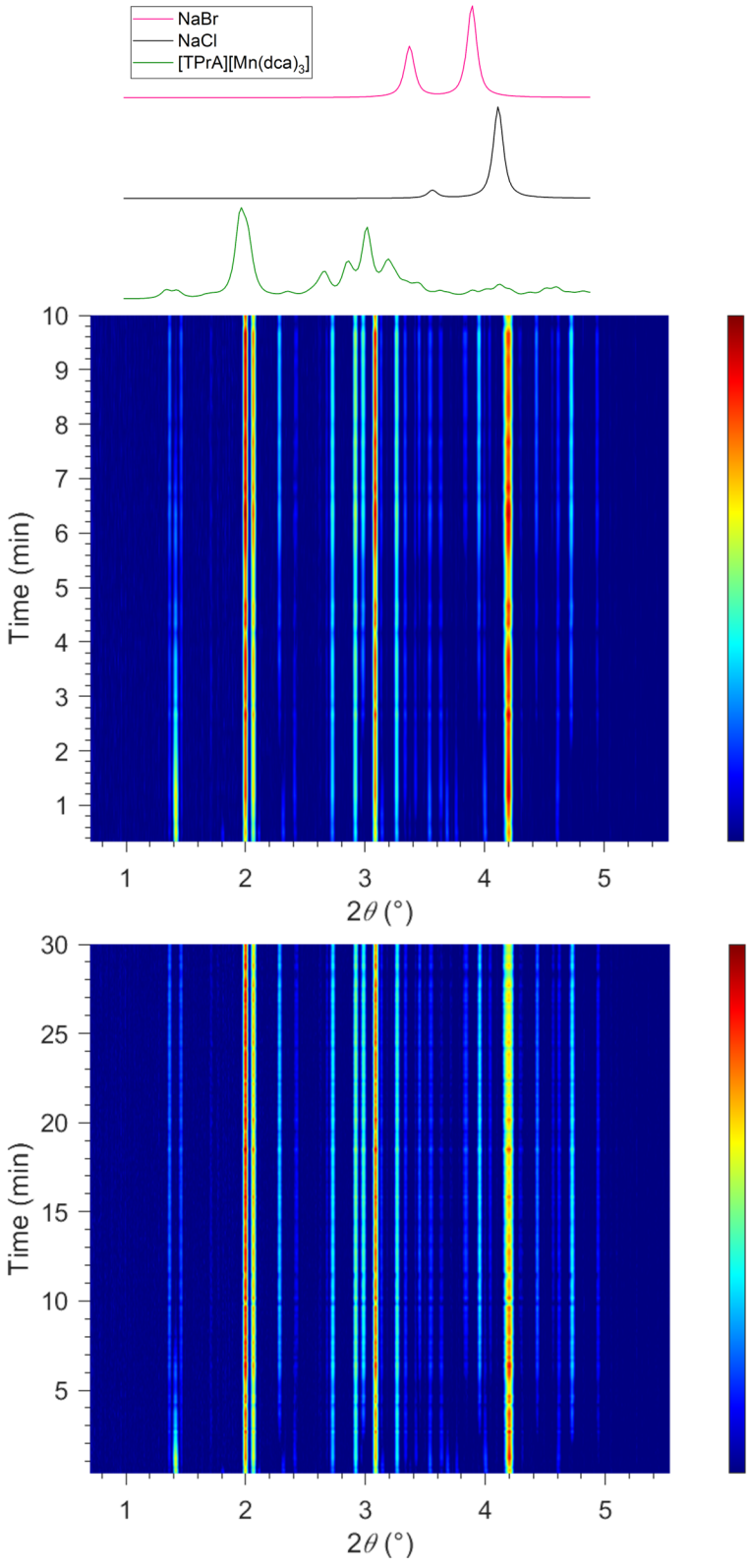

Figure S6. *In situ* PXRD of [TPrA][Mn(dca)$_3$], showing that the material forms within 10 minutes and no further changes are observed after 30 minutes of synthesis. Red = areas of high intensity and blue = areas of low intensity. Simulated PXRD patterns of [TPrA][Mn(dca)$_3$], NaCl and NaBr are shown for clarity.

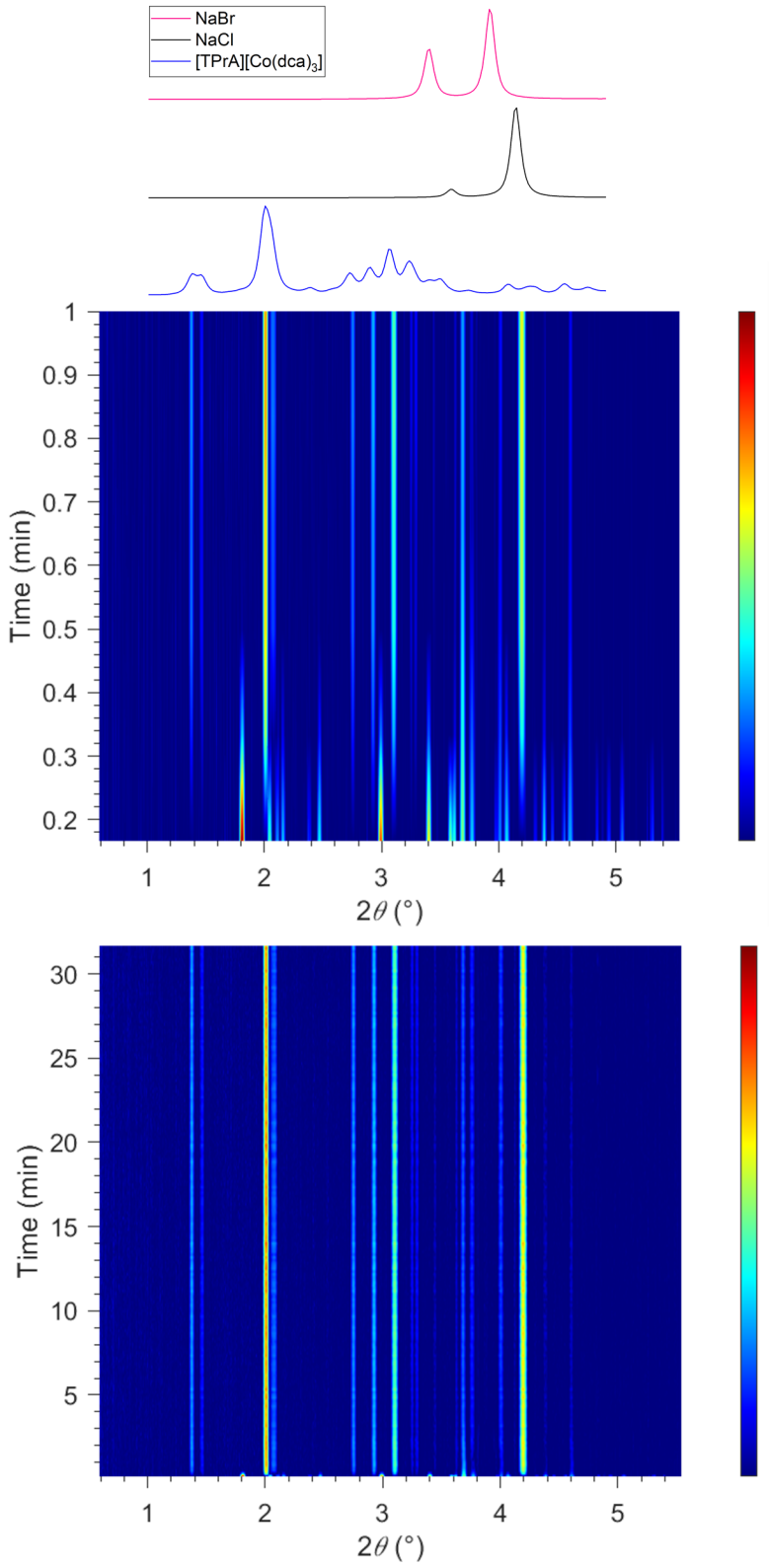

Figure S7. *In situ* PXRD of [TPrA][Co(dca)$_3$], showing that (a) the material forms after *ca.* 30 seconds and (b) no further changes are observed after 30 minutes of synthesis. Red = areas of high intensity and blue = areas of low intensity. Simulated PXRD patterns of [TPrA][Co(dca)$_3$], NaCl and NaBr are shown for clarity.

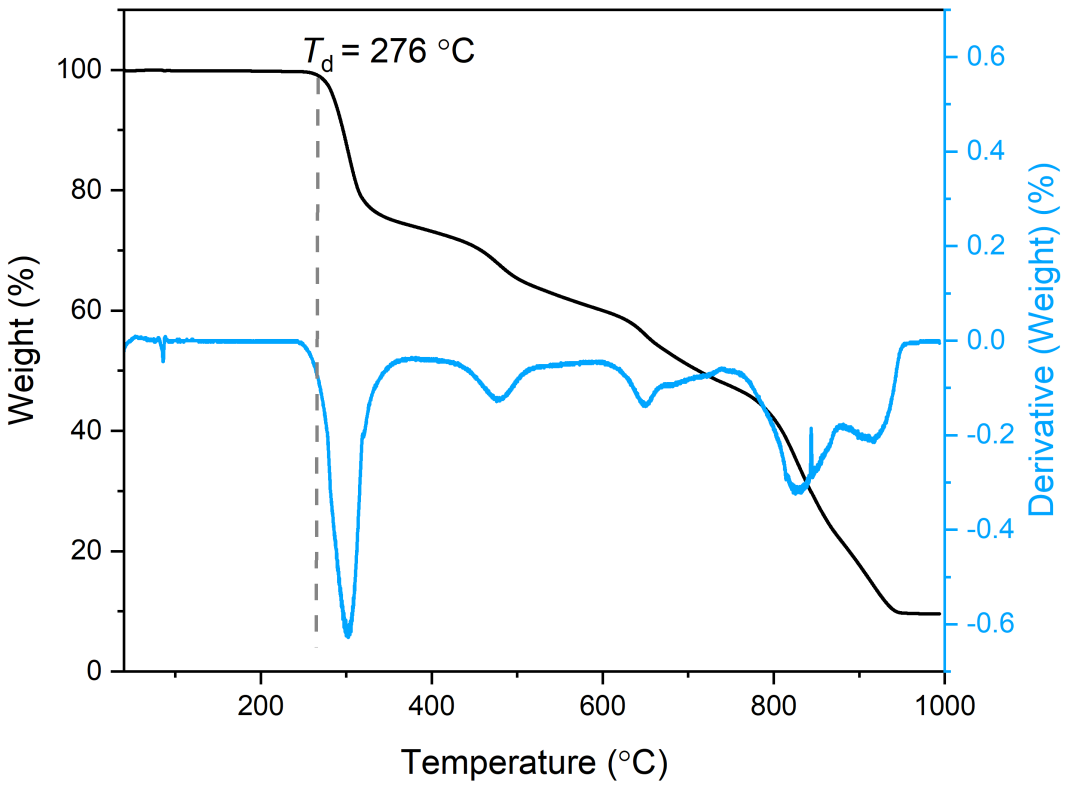

Figure S8. TGA curve showing the change in weight % (black trace), and plot of the derivative weight % (blue trace) with increasing temperature for [TPrA][Mn(dca)$_3$]. Measured at 10 ºC min^{-1} under an Ar atmosphere. The dashed line (grey) represents the decomposition temperature (T_d), recorded as 276 ºC.

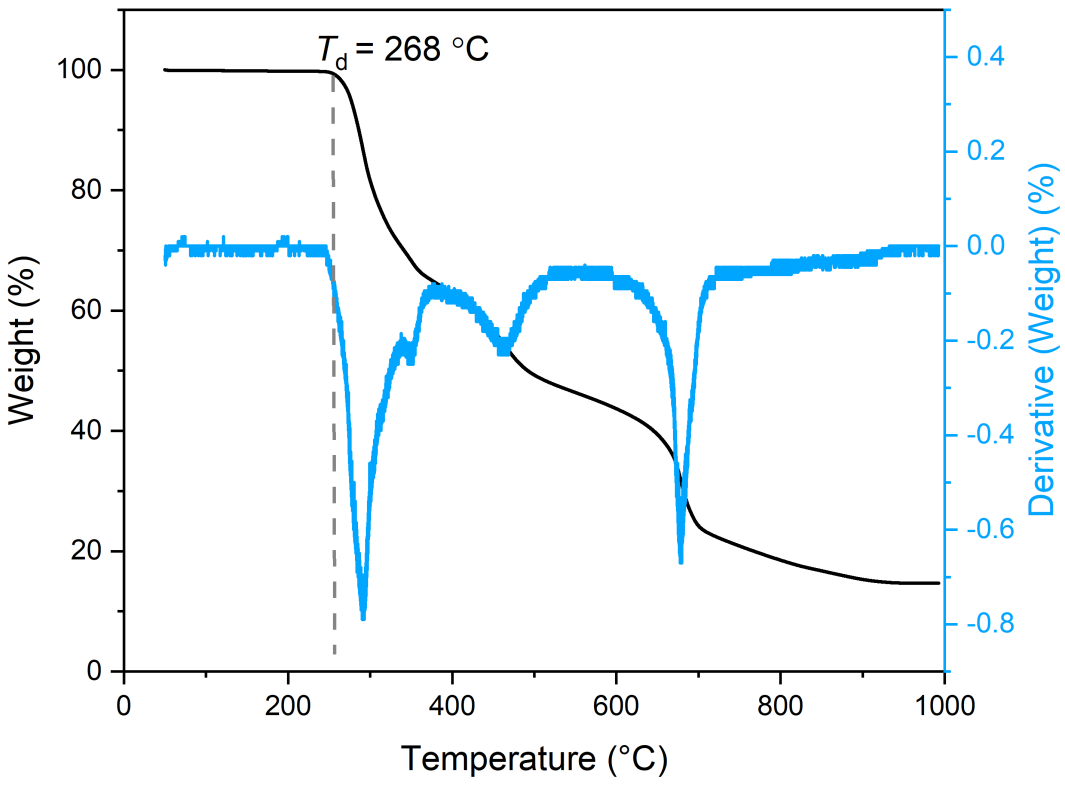

Figure S9. TGA curve showing the change in weight % (black trace), and plot of the derivative weight % (blue trace) with increasing temperature for [TPrA][Mn(dca)$_3$]. Measured at 10 ºC min^{-1} under an N_2 atmosphere. The dashed line (grey) represents the decomposition temperature (T_d), recorded as 268 ºC.

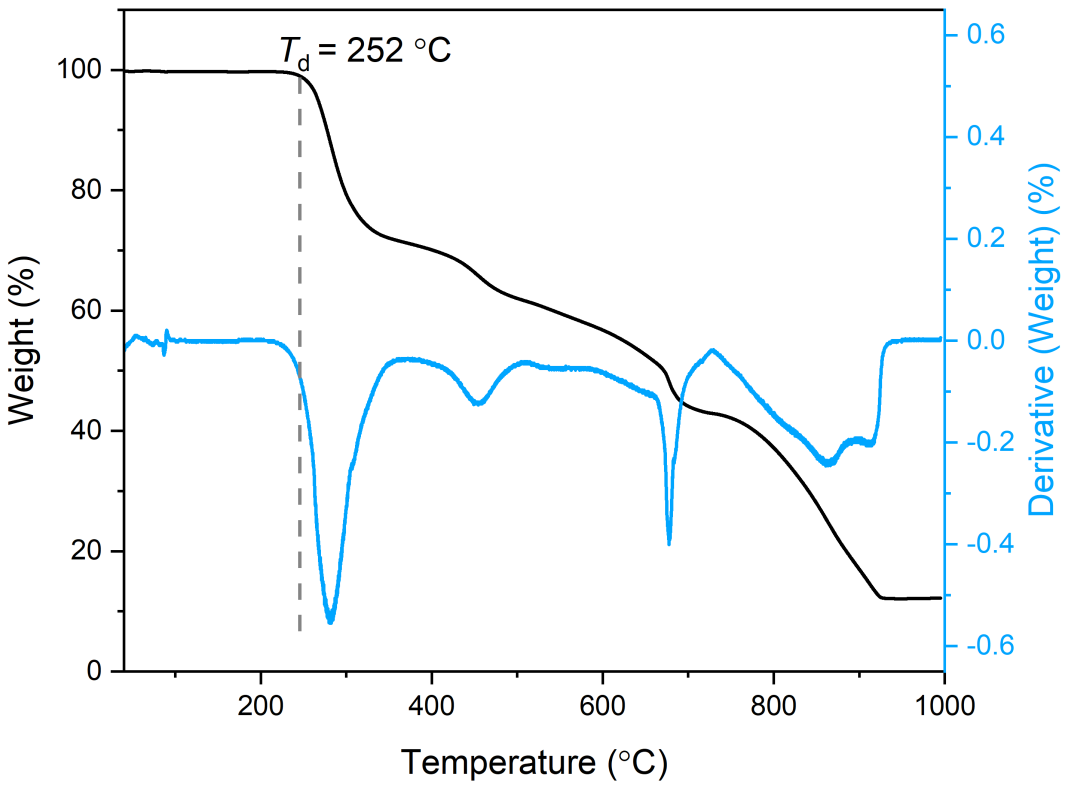

Figure S10. TGA curve showing the change in weight % (black trace), and plot of the derivative weight % (blue trace) with increasing temperature for [TPrA][Co(dca)$_3$]. Measured at 10 ºC min^{-1} under an Ar atmosphere. The dashed line (grey) represents the decomposition temperature (T_d), recorded as 252 ºC.

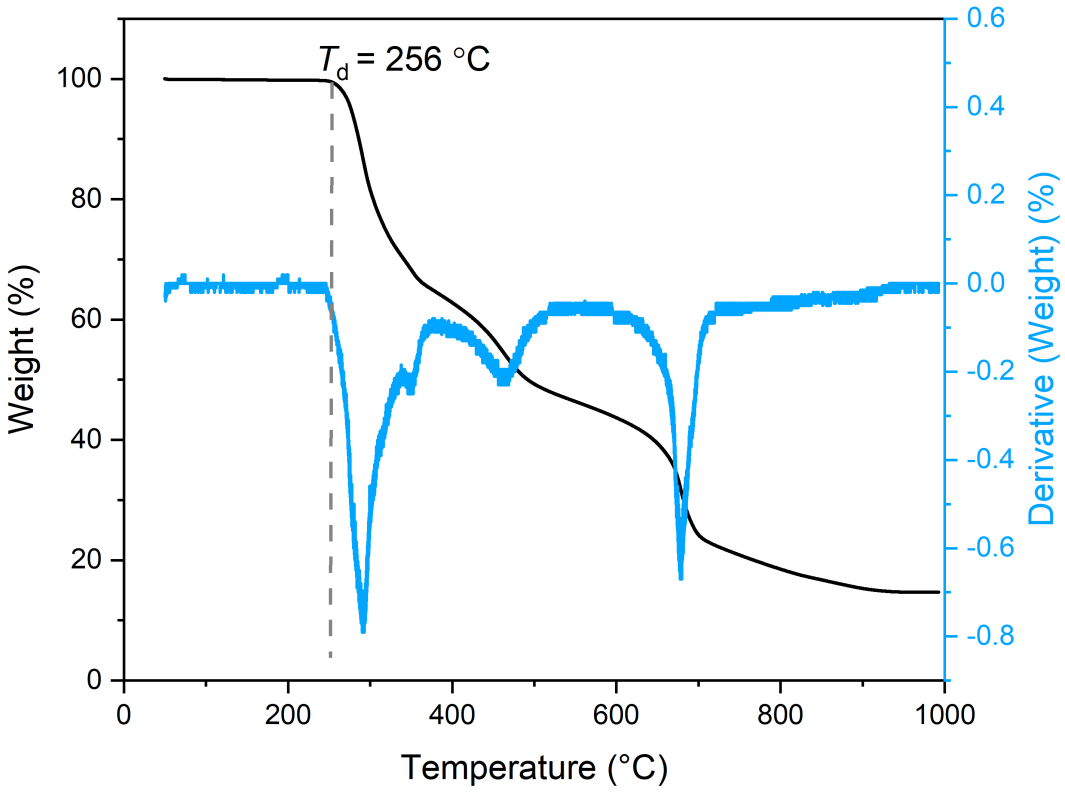

Figure S11. TGA curve showing the change in weight % (black trace), and plot of the derivative weight % (blue trace) with increasing temperature for [TPrA][Co(dca)$_3$]. Measured at 10 ºC min^{-1} under an N_2 atmosphere. The dashed line (grey) represents the decomposition temperature (T_d), recorded as 256 ºC.

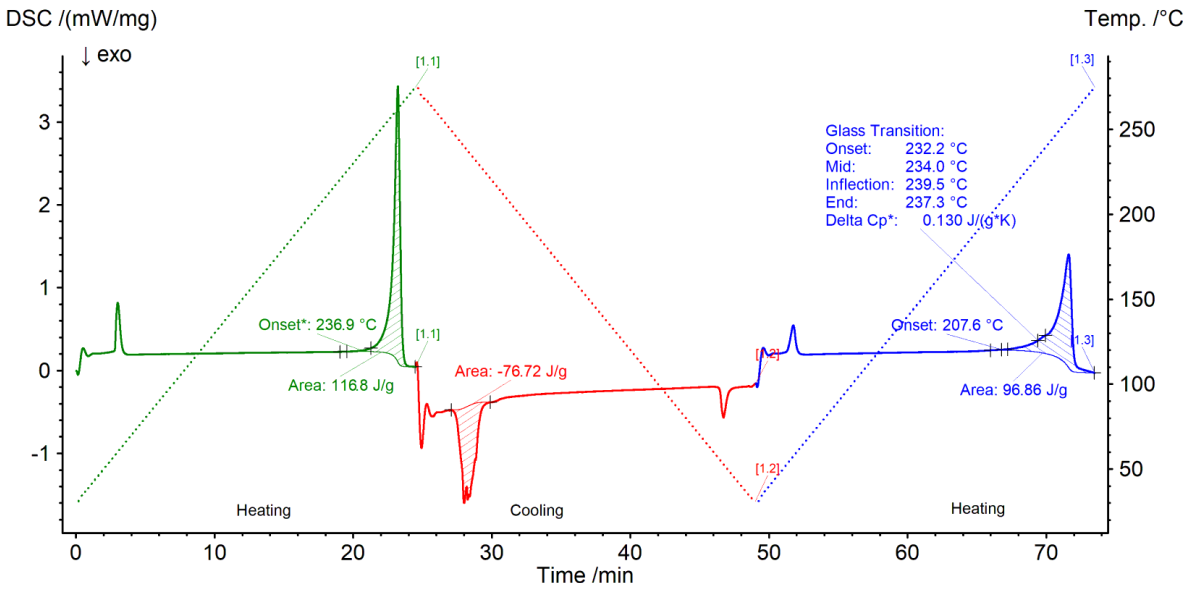

Figure S12. Full DSC scan of [TPrA][Mn(dca)$_3$], where the sample was heated to 275 ºC at 10 °C min^{-1}, then cooled to 30 ºC at 10 ºC min^{-1} and then heated again to 275 ºC at 10 ºC min^{-1}. The melting temperature (T_m) was recorded as 237 ºC and the glass transition temperature (T_g) was recorded as 232 ºC. Significant recrystallisation was evident in the sample upon cooling. The small feature evident at 50-60 ºC on both the up and down-scans are from previously reported polymorphic solid-solid phase transitions.[6]

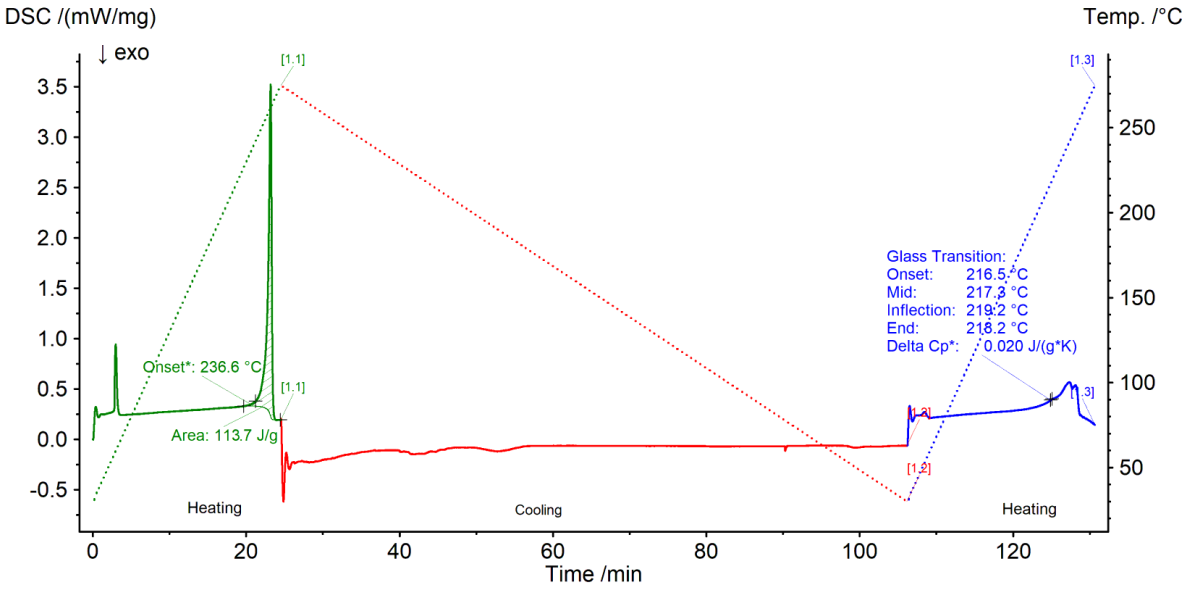

Figure S13. Full DSC scan of [TPrA][Mn(dca)$_3$], where the sample was heated to 275 ºC at 10 ºC min^{-1}, then cooled to 30 ºC at 3 ºC min^{-1} and then heated again to 275 ºC at 10 ºC min^{-1}. The T_m was recorded as 237 ºC and the T_g was recorded as 217 ºC. Little to no recrystallisation was evident in the sample upon cooling. The small feature evident at 50-60 ºC on both the up and down-scans are from previously reported polymorphic solid-solid phase transitions.[6]

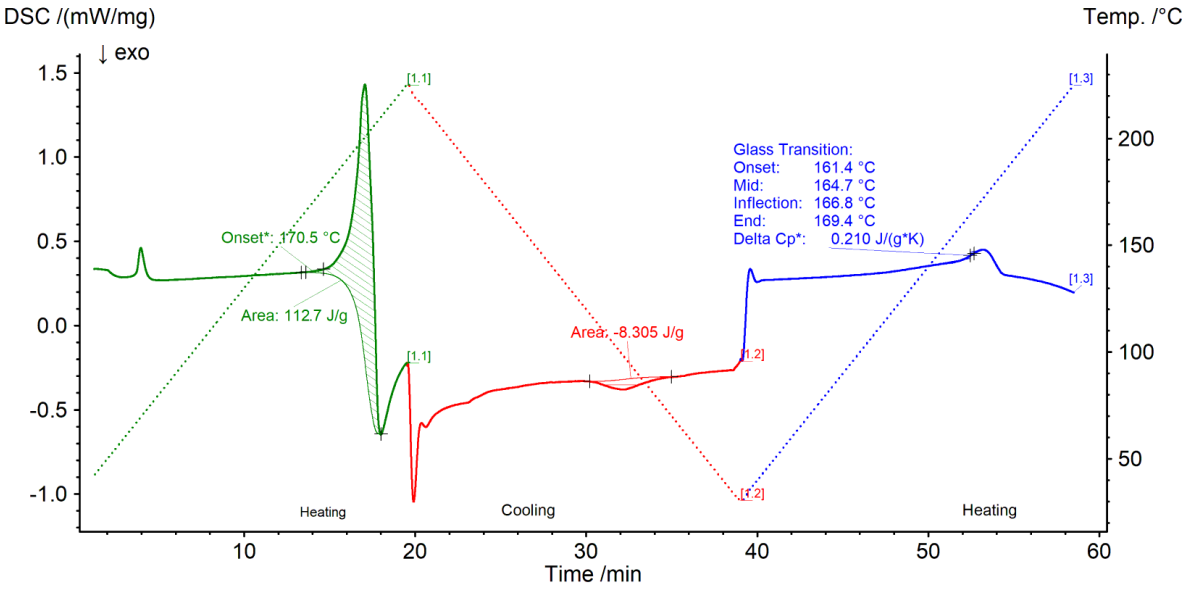

Figure S14. Full DSC scan of [TPrA][Co(dca)$_3$], where the sample was heated to 225 ºC at 10 ºC min^{-1}, then cooled to 30 ºC at 10 ºC min^{-1} and then heated again to 225 ºC at 10 ºC min^{-1}. The T_m was recorded as 171 ºC, and the T_g was recorded as 161 ºC. Minor recrystallisation was evident upon cooling. The small feature evident at 60-70 ºC on the first up-scan represents a previously reported polymorphic solid-solid phase transition.[7]

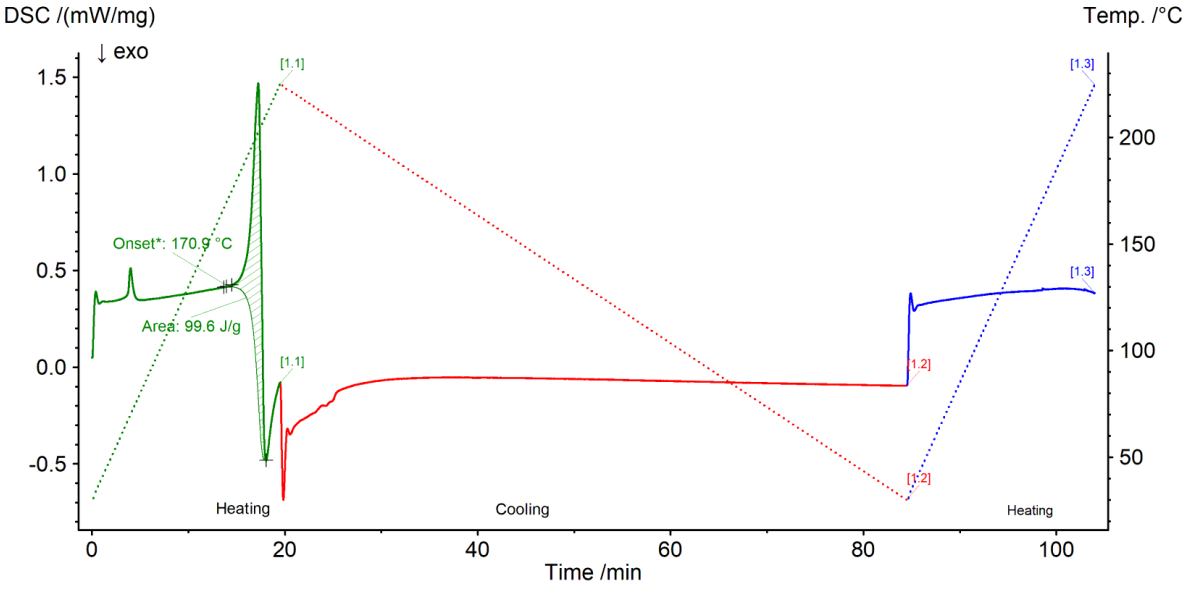

Figure S15. Full DSC scan of [TPrA][Co(dca)$_3$], where the sample was heated to 225 ºC at 10 ºC min^{-1}, then cooled to 30 ºC at 3 ºC min^{-1} and then heated again to 225 ºC at 10 ºC min^{-1}. The T_m was recorded as 171 ºC, though no T_g was observed. No recrystallisation was evident in the sample upon cooling. The small feature evident at 60-70 ºC on the first up-scan represents a previously reported polymorphic solid-solid phase transition.[7]

Table S1. T_m onsets, T_g onsets, T_ds and associated literature values of HOIP samples (denoted by *).[8]

Sample	T_m onset (Ar) (ºC)	T_g onset (Ar) cooled at 10 ºC min^{-1} (ºC)	T_d (Ar) (ºC)
[TPrA][Mn(dca)$_3$]	237 **255*	232 **218*	276 **281*
		T_g onset (Ar) cooled at 3 ºC min^{-1} (ºC)	
		217	
	T_m onset (N_2) (ºC)	**T_g onset (N_2) cooled at 10 ºC min^{-1} (ºC)**	**T_d (N_2) (ºC)**
	240	221	268
[TPrA][Co(dca)$_3$]	**T_m onset (Ar) (ºC)**	**T_g onset (Ar) (ºC)**	**T_d (Ar) (ºC)**
	171 **205*	161 **125*	252 **267*
		T_g onset (Ar) cooled at 3 ºC min^{-1} (ºC)	
		N/A	
	T_m onset (N_2) (ºC)	**T_g onset (N_2) (ºC)**	**T_d (N_2) (ºC)**
	173	160	256

a.

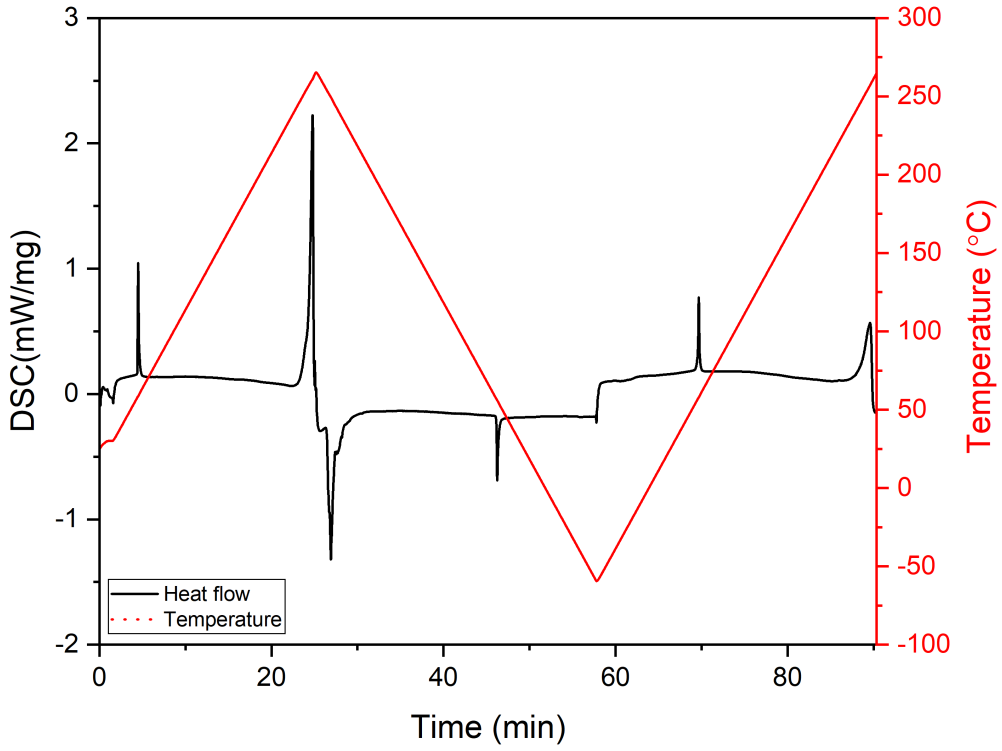

b.

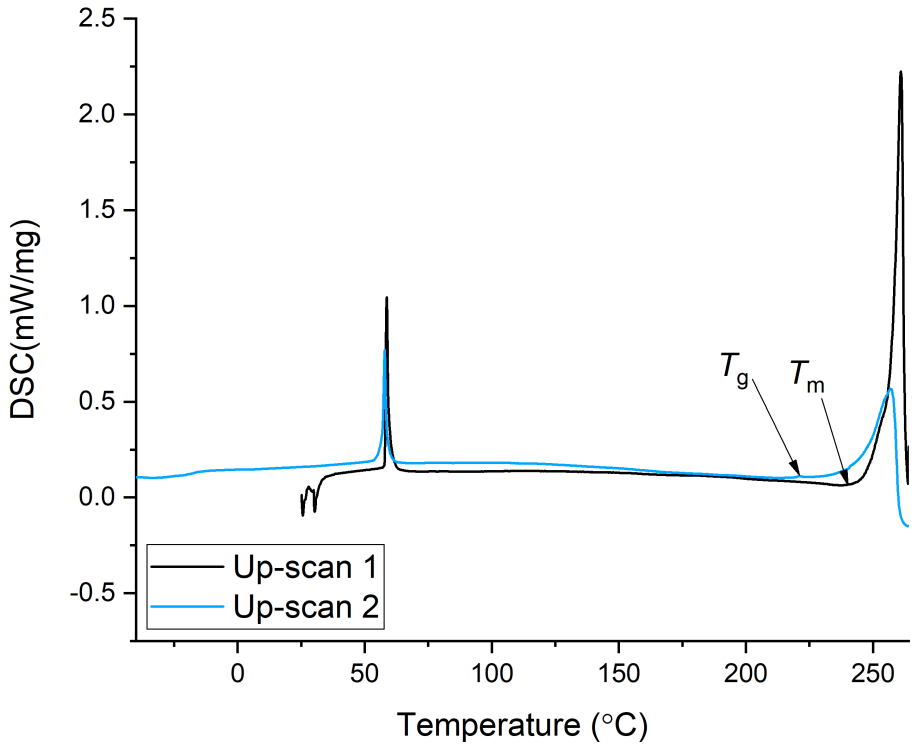

Figure S16. (a) Full low-temperature DSC scan of [TPrA][Mn(dca)$_3$], where the sample was heated to 266 ºC at 10 ºC min^{-1}, then cooled to -60 ºC at 10 ºC min^{-1} and then heated again to 266 ºC at 10 ºC min^{-1}. (b) Up-scans 1 and 2 showing the T_m (240 ºC) and the T_g (221 ºC).

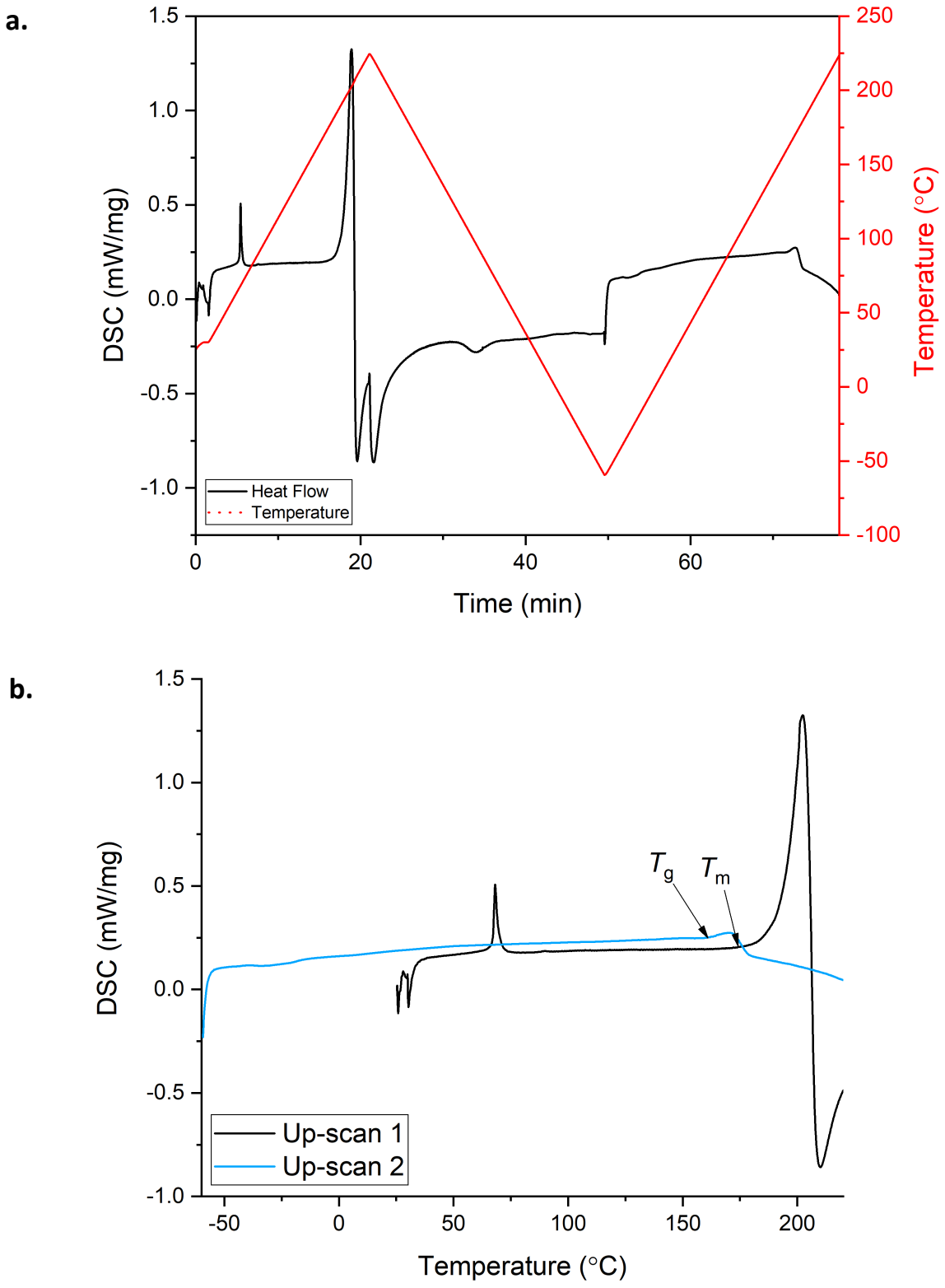

Figure S17. (a) Full low-temperature DSC scan of [TPrA][Co(dca)$_3$], where the sample was heated to 225 ºC at 10 ºC min^{-1}, then cooled to -60 ºC at 10 ºC min^{-1} and then heated again to 225 ºC at 10 ºC min^{-1}. (b) Up-scans 1 and 2 showing the T_m (173 ºC) and the T_g (160 ºC).

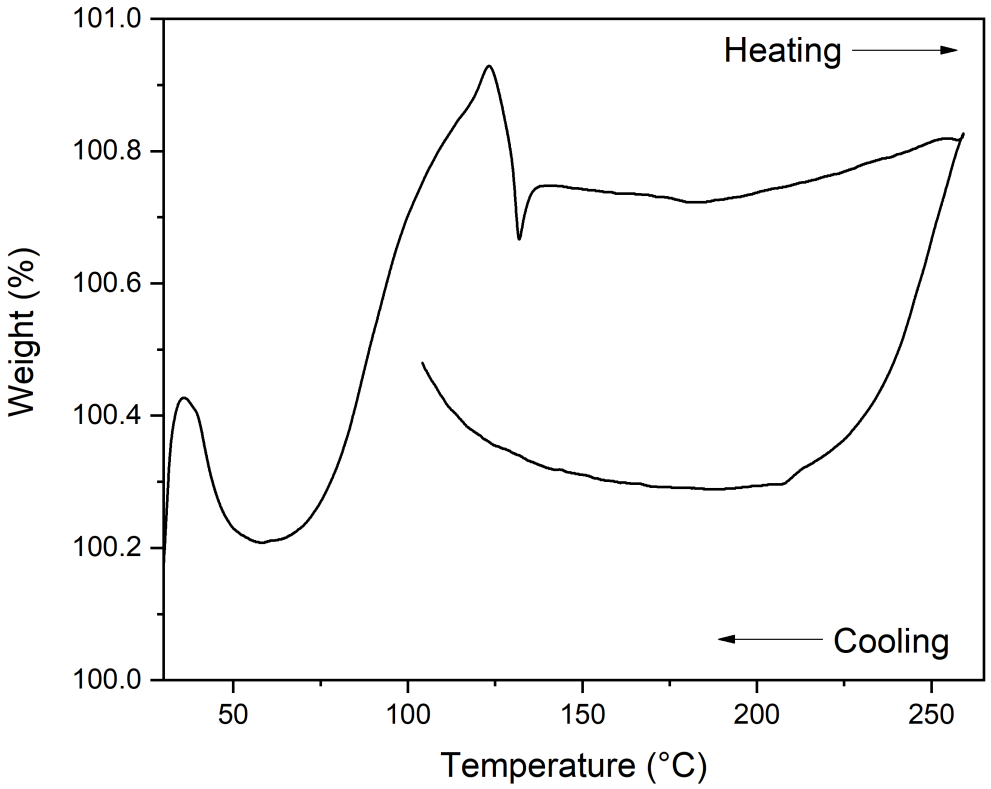

Figure S18. TGA curve showing the change in weight % with increasing and decreasing temperature for [TPrA][Mn(dca)$_3$]. Heated from 30 ºC to 260 ºC at 10 ºC min^{-1}, then cooled at 10 ºC min^{-1} under an Ar atmosphere.

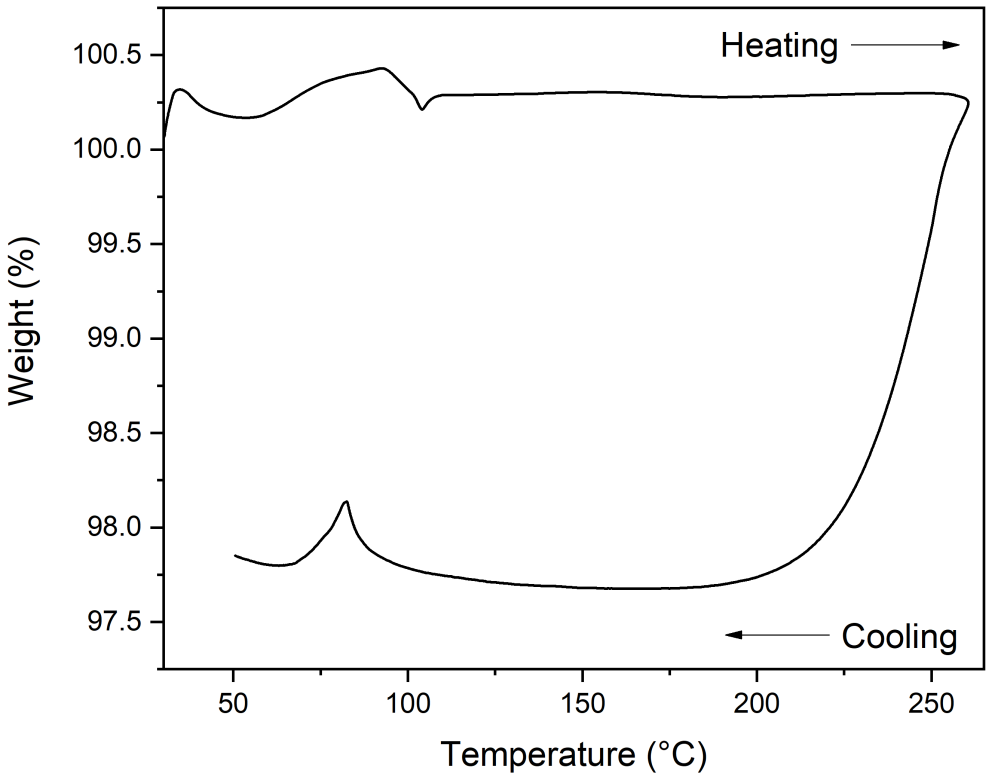

Figure S19. TGA curve showing the change in weight % with increasing and decreasing temperature for [TPrA][Mn(dca)$_3$]. Heated from 30 ºC to 260 ºC at 10 ºC min^{-1}, then cooled at 3 ºC min^{-1} under an Ar atmosphere.

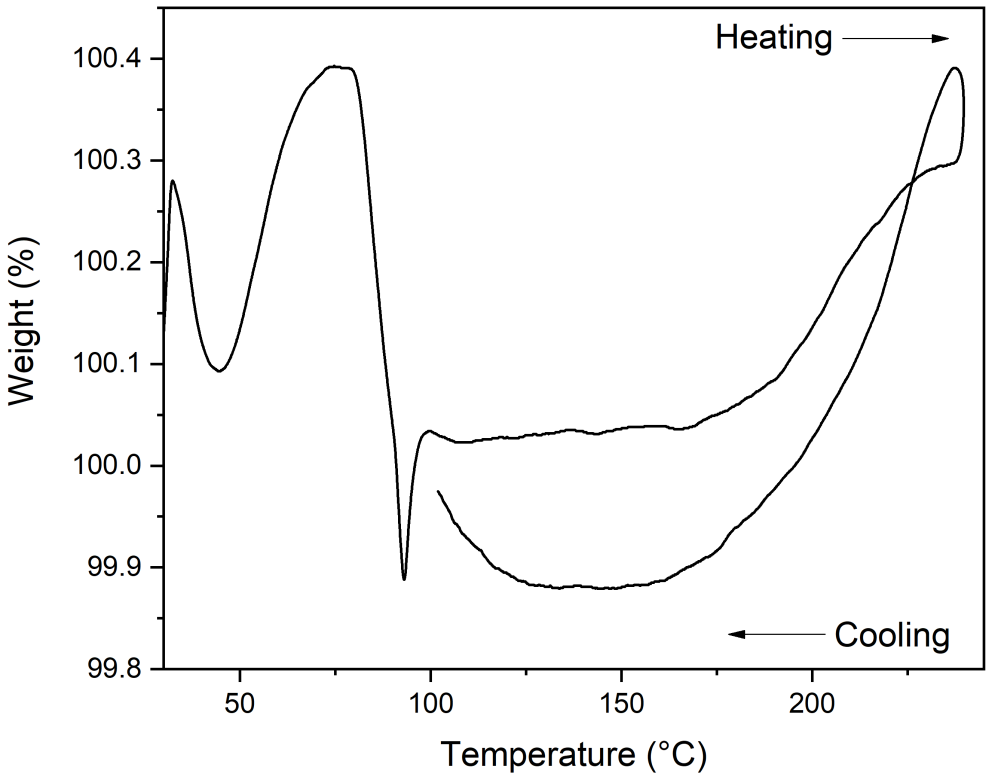

Figure S20. TGA curve showing the change in weight % with increasing and decreasing temperature for [TPrA][Co(dca)$_3$]. Heated from 30 ºC to 240 ºC at 10 ºC min^{-1}, then cooled at 10 ºC min^{-1} under an Ar atmosphere.

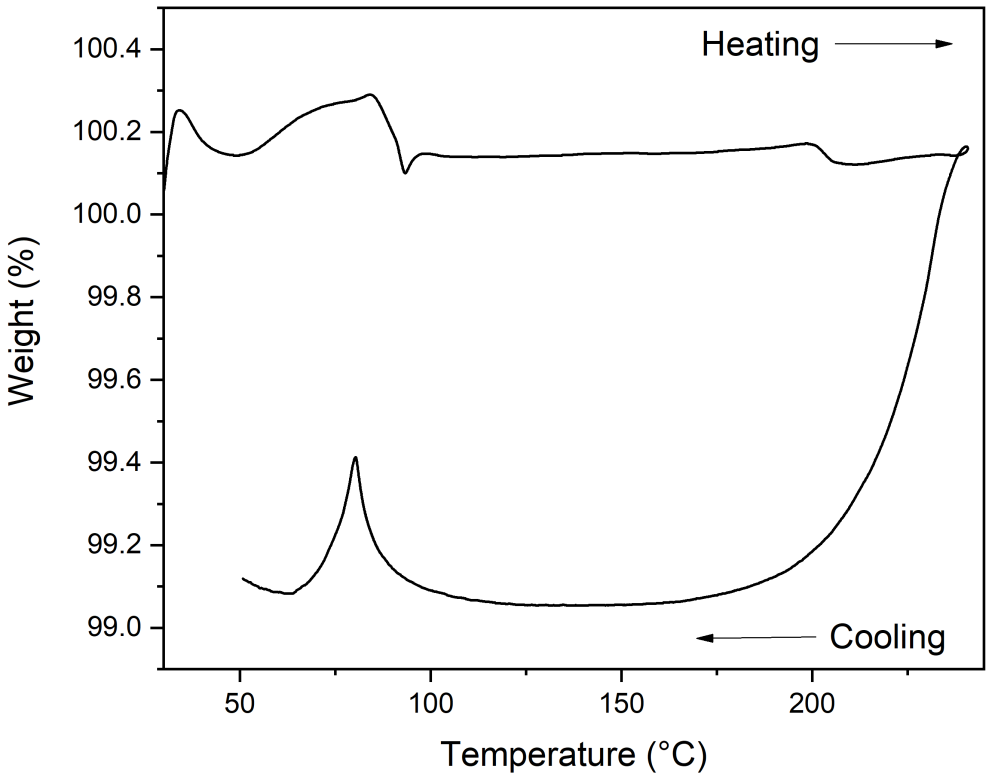

Figure S21. TGA curve showing the change in weight % with increasing and decreasing temperature for [TPrA][Co(dca)$_3$]. Heated from 30 ºC to 240 ºC at 10 ºC min^{-1}, then cooled at 3 ºC min^{-1} under an Ar atmosphere.

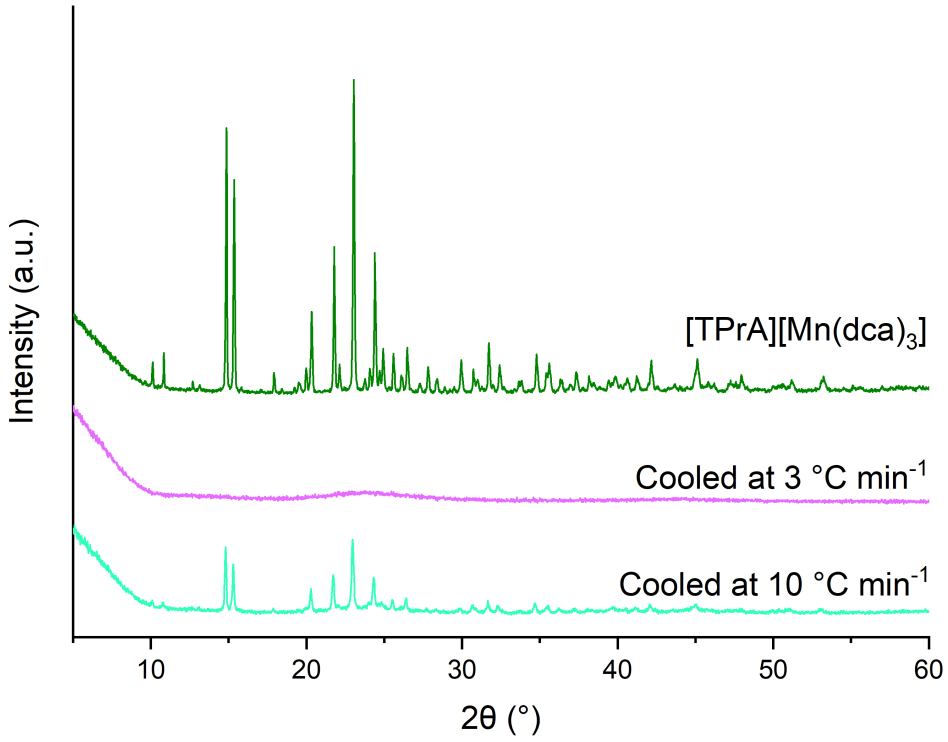

Figure S22. PXRD patterns of as-made [TPrA][Mn(dca)$_3$] and after heating and cooling in an SDT, where samples were heated to 260 ºC at 10 ºC min^{-1}, then cooled to 30 ºC at either 10 ºC min^{-1} or 3 ºC min^{-1}, to investigate the effect of cooling rate on recrystallisation in the material. The resulting a_g[TPrA][Mn(dca)$_3$] is amorphous when cooled at 3 ºC min^{-1}, though partially recrystallises when cooled at the faster rate of 10 ºC min^{-1}.

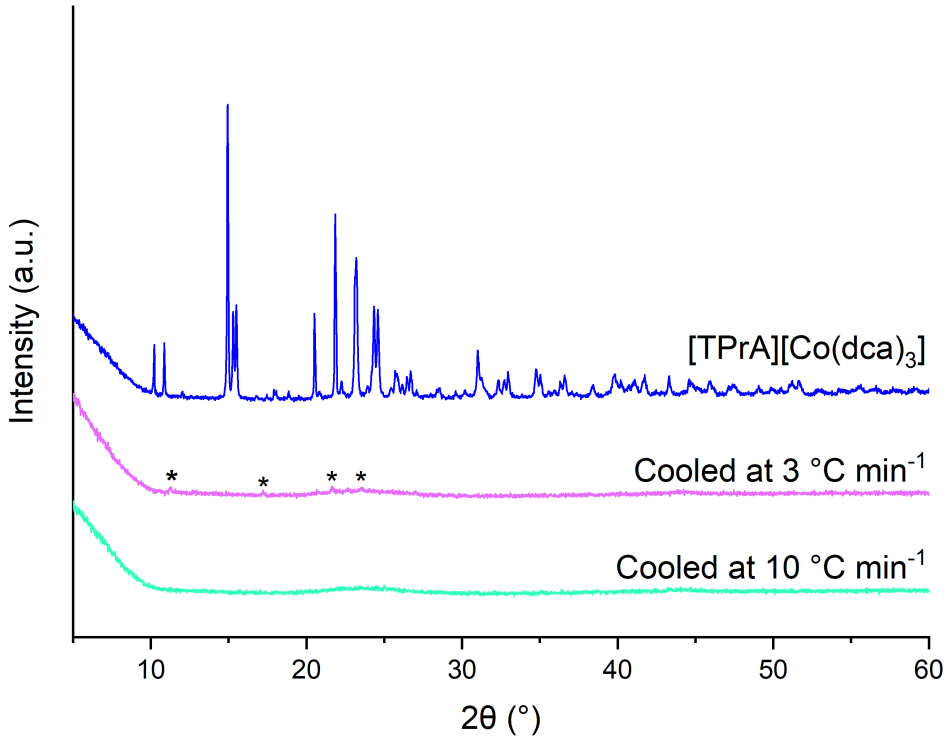

Figure S23. PXRD patterns of as-made [TPrA][Co(dca)$_3$] and after heating and cooling in an SDT, where samples were heated to 240 ºC at 10 ºC min^{-1}, then cooled to 30 ºC at either 10 ºC min^{-1} or 3 ºC min^{-1}, to investigate the effect of cooling rate on recrystallisation in the material. The resulting a_g[TPrA][Co(dca)$_3$] is amorphous when cooled at both 10 ºC min^{-1} and 3 ºC min^{-1}, though extremely minor impurity Bragg peaks (marked with an asterisk) are evident in the sample cooled at 3 ºC min^{-1}.

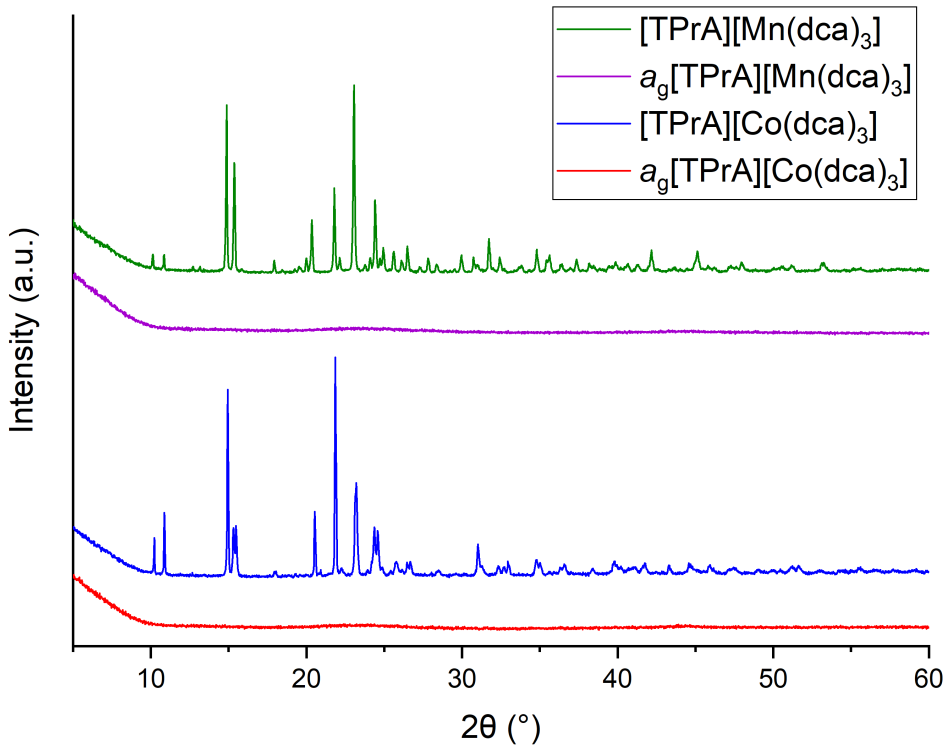

Figure S24. PXRD patterns of both the crystalline and bulk glass forms of [TPrA][Mn(dca)$_3$] and [TPrA][Co(dca)$_3$].

Table S2. CHN microanalysis of crystalline and glass HOIP samples, glass samples recovered from aqueous solutions (pH2-10) and the unknown crystalline phases (pH13).

Sample:	%C	%H	%N
[TPrA][Co(dca)$_3$]	47.78	6.19	30.64
a_g[TPrA][Co(dca)$_3$]	42.28	5.30	29.99
a_g[TPrA][Co(dca)$_3$] pH2	26.30	2.78	32.00
a_g[TPrA][Co(dca)$_3$] pH5	27.19	3.17	30.78
a_g[TPrA][Co(dca)$_3$] pH7	29.35	3.60	30.53
a_g[TPrA][Co(dca)$_3$] pH10	28.81	3.48	29.06
a_g[TPrA][Co(dca)$_3$] pH13	10.97	1.77	7.65
[TPrA][Mn(dca)$_3$]	48.95	6.21	31.03
a_g[TPrA][Mn(dca)$_3$]	33.85	4.07	33.55
a_g[TPrA][Mn(dca)$_3$] pH2	26.67	2.66	34.63
a_g[TPrA][Mn(dca)$_3$] pH5	25.89	2.73	32.92
a_g[TPrA][Mn(dca)$_3$] pH7	26.76	2.90	33.09
a_g[TPrA][Mn(dca)$_3$] pH10	25.85	2.68	33.23
a_g[TPrA][Mn(dca)$_3$] pH13	7.55	1.13	2.45

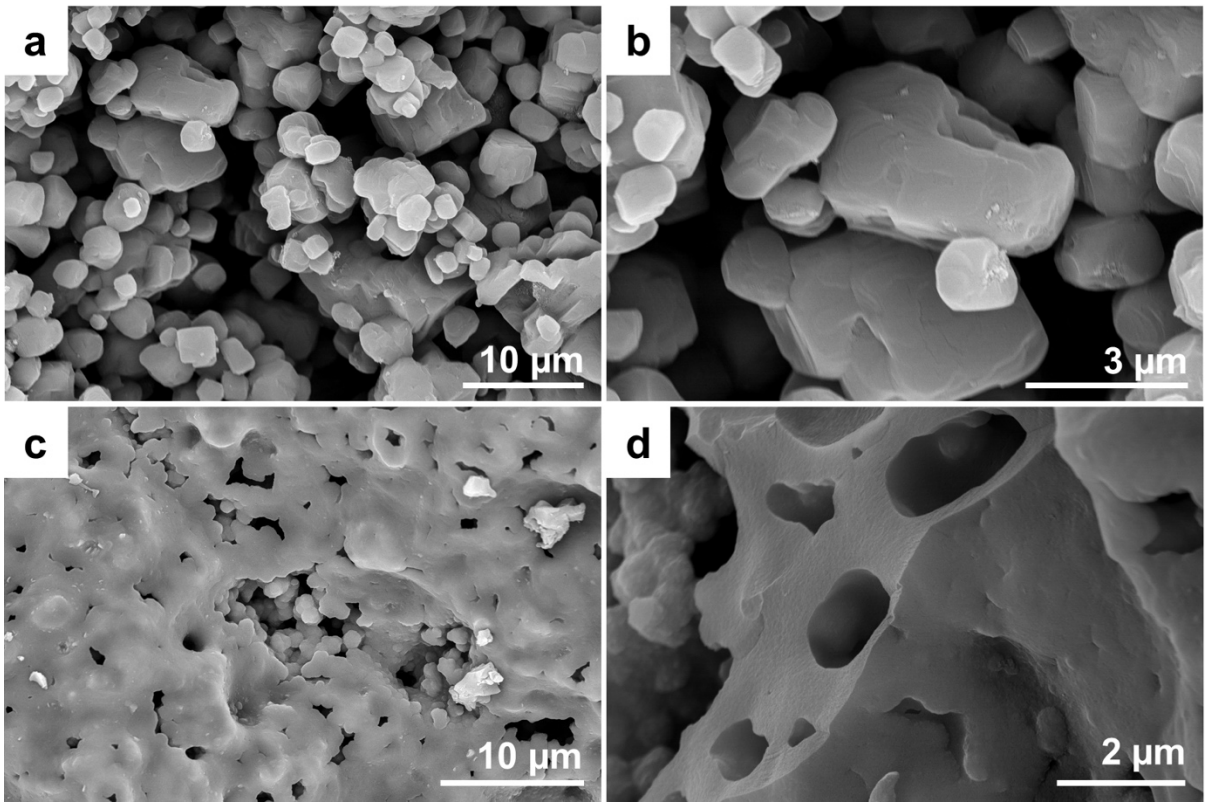

Figure S25. SEM images of (a and b) [TPrA][Mn(dca)$_3$], where the crystalline material consists of rounded, block-shaped crystals. (c and d) a_g[TPrA][Mn(dca)$_3$], where flow is evident in the glass sample and surface porosity is clearly visible.

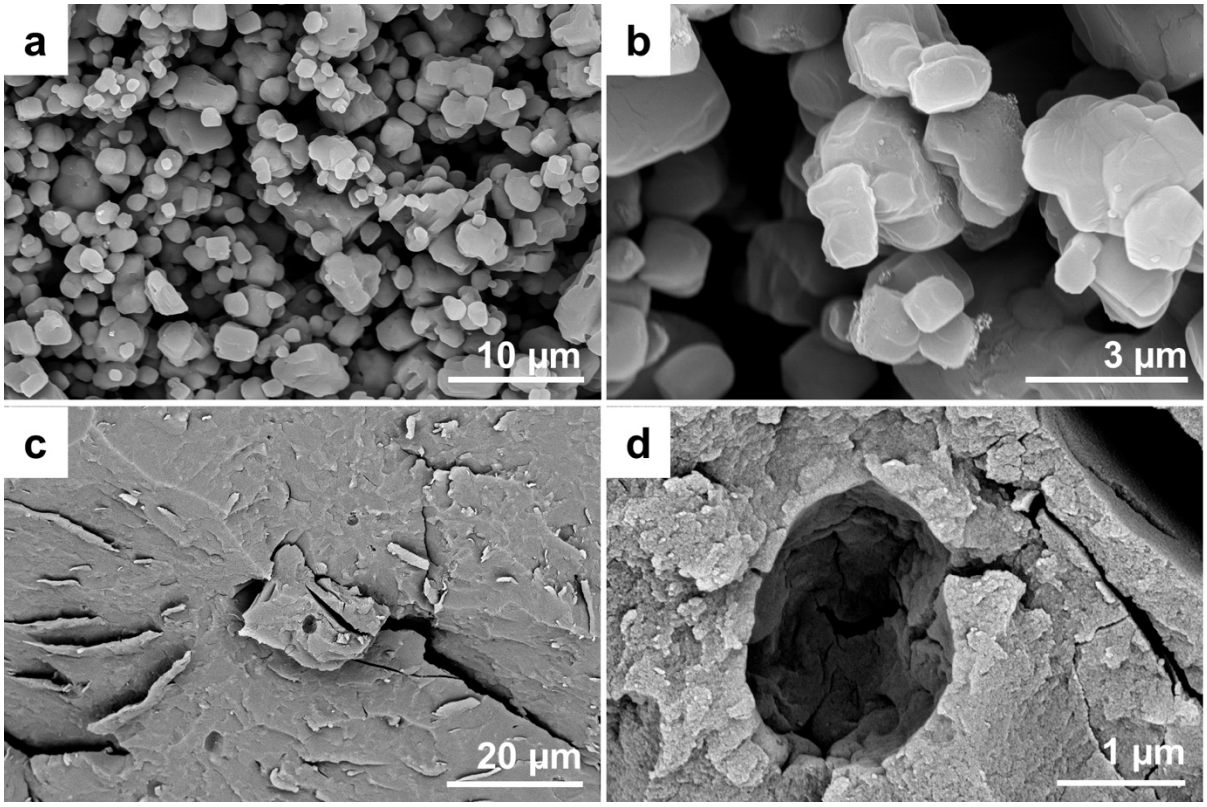

Figure S26. SEM images of (a and b) [TPrA][Co(dca)$_3$], where the crystalline material consists of rounded, block-shaped crystals. (c and d) a_g[TPrA][Co(dca)$_3$], where significant flow is evident in the glass sample and minor surface porosity is visible.

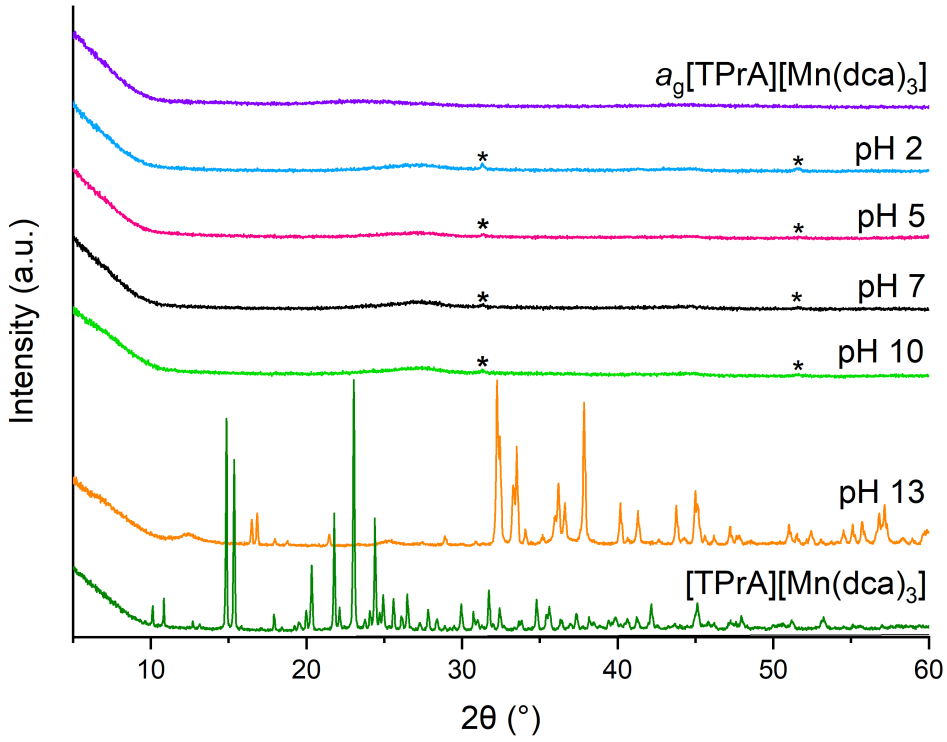

Figure S27. PXRD patterns of as-made a_g[TPrA][Mn(dca)$_3$] and after exposure to aqueous solutions, ranging from strongly acidic to strongly basic, for seven days. Samples exposed to pH 2-10 remained amorphous, with no recrystallisation to the original crystalline phase ([TPrA][Mn(dca)$_3$]), though very minor impurity Bragg peaks were evident (marked with an asterisk). A crystalline sample of unknown origin was recovered from a strongly basic solution (pH 13).

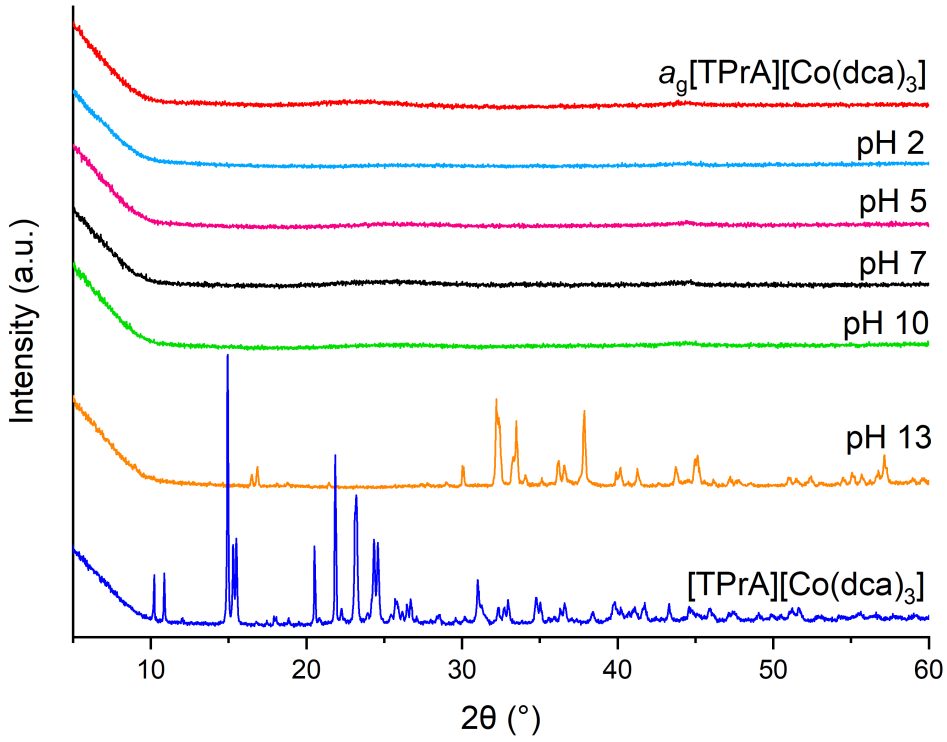

Figure S28. PXRD patterns of as-made a_g[TPrA][Co(dca)$_3$] and after exposure to aqueous solutions, ranging from strongly acidic to strongly basic, for seven days. Samples exposed to pH 2-10 remained amorphous and no recrystallisation to the original crystalline phase ([TPrA][Co(dca)$_3$]) was observed. A crystalline sample of unknown origin was recovered from a strongly basic solution (pH 13).

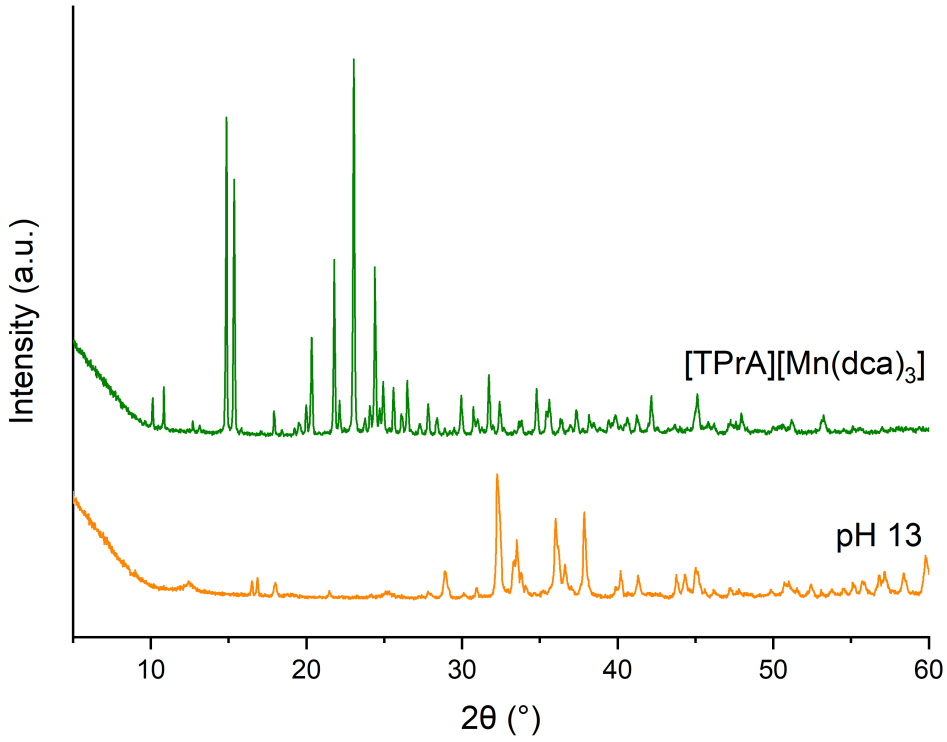

Figure S29. PXRD patterns of as-made [TPrA][Mn(dca)$_3$] and after exposure to a strongly basic aqueous solution (pH 13) for seven days. A crystalline sample of unknown origin was recovered from the solution.

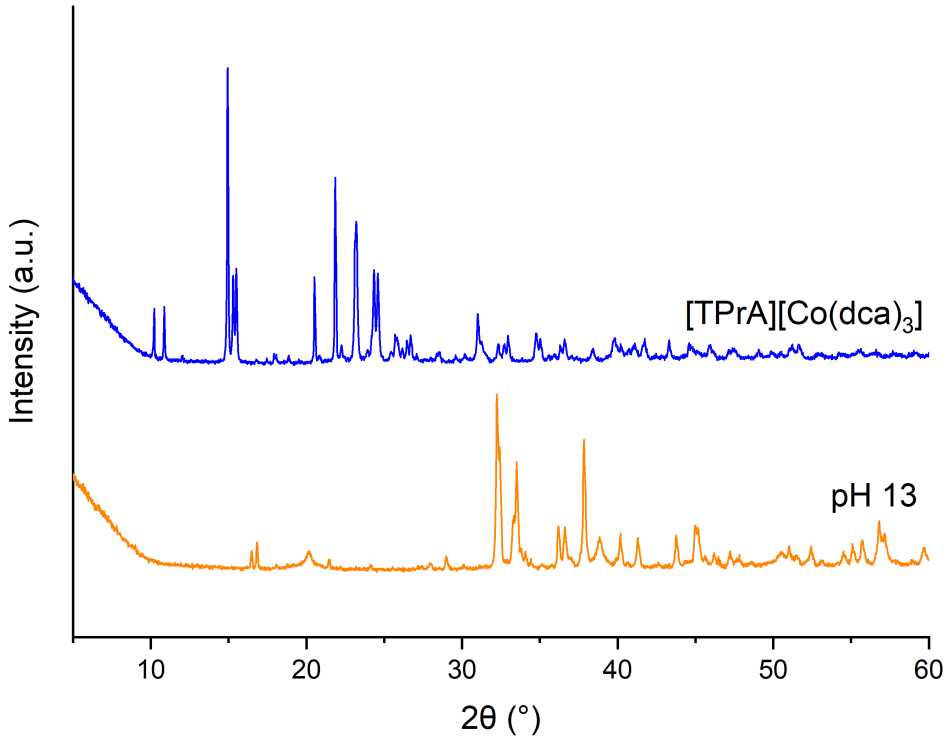

Figure S30. PXRD patterns of as-made [TPrA][Co(dca)$_3$] and after exposure to a strongly basic aqueous solution (pH 13) for seven days. A crystalline sample of unknown origin was recovered from the solution.

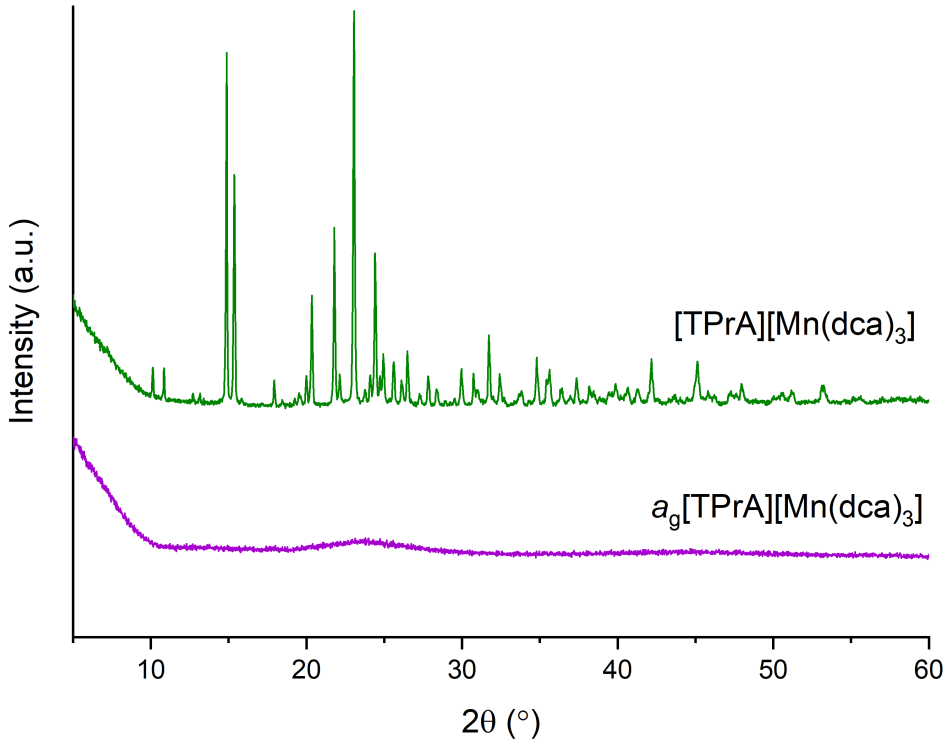

Figure S31. PXRD patterns of as-made [TPrA][Mn(dca)$_3$] and after melting a pelletised sample in an alumina crucible. No recrystallisation is evident in the sample.

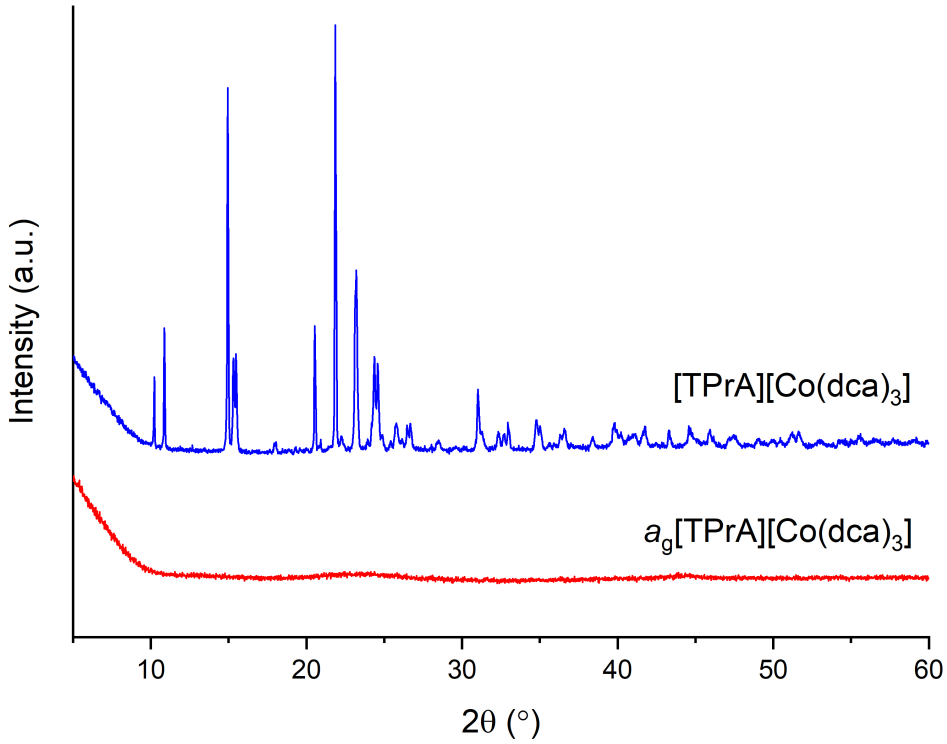

Figure S32. PXRD patterns of as-made [TPrA][Co(dca)$_3$] and after melting a pelletised sample in an alumina crucible. No recrystallisation is evident in the sample.

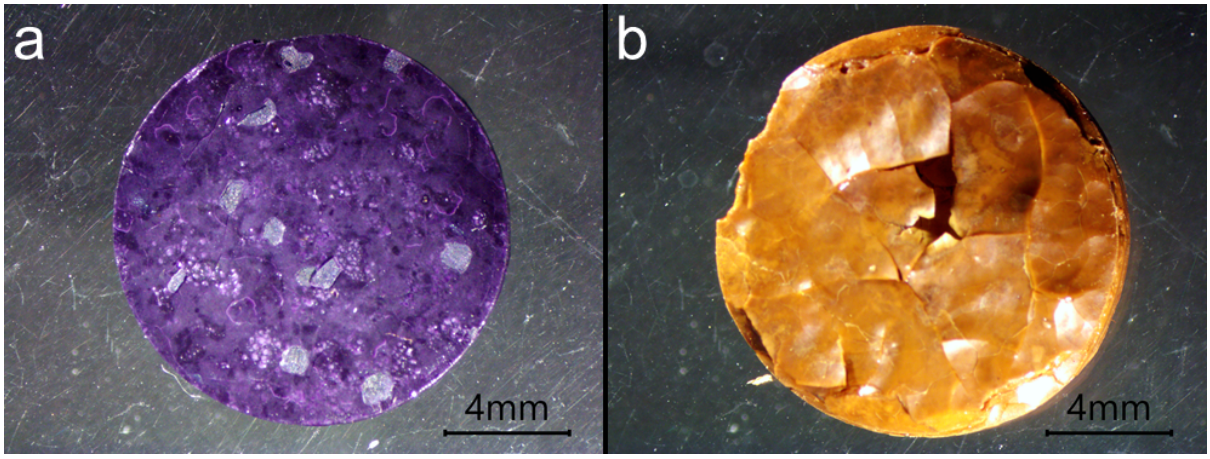

Figure S33. Pellets of (a) a_g[TPrA][Co(dca)$_3$] and (b) a_g[TPrA][Mn(dca)$_3$]. The surface of the a_g[TPrA][Co(dca)$_3$] pellet was found to be relatively smooth, while the pelletised a_g[TPrA][Mn(dca)$_3$] sample was very 'flaky'.

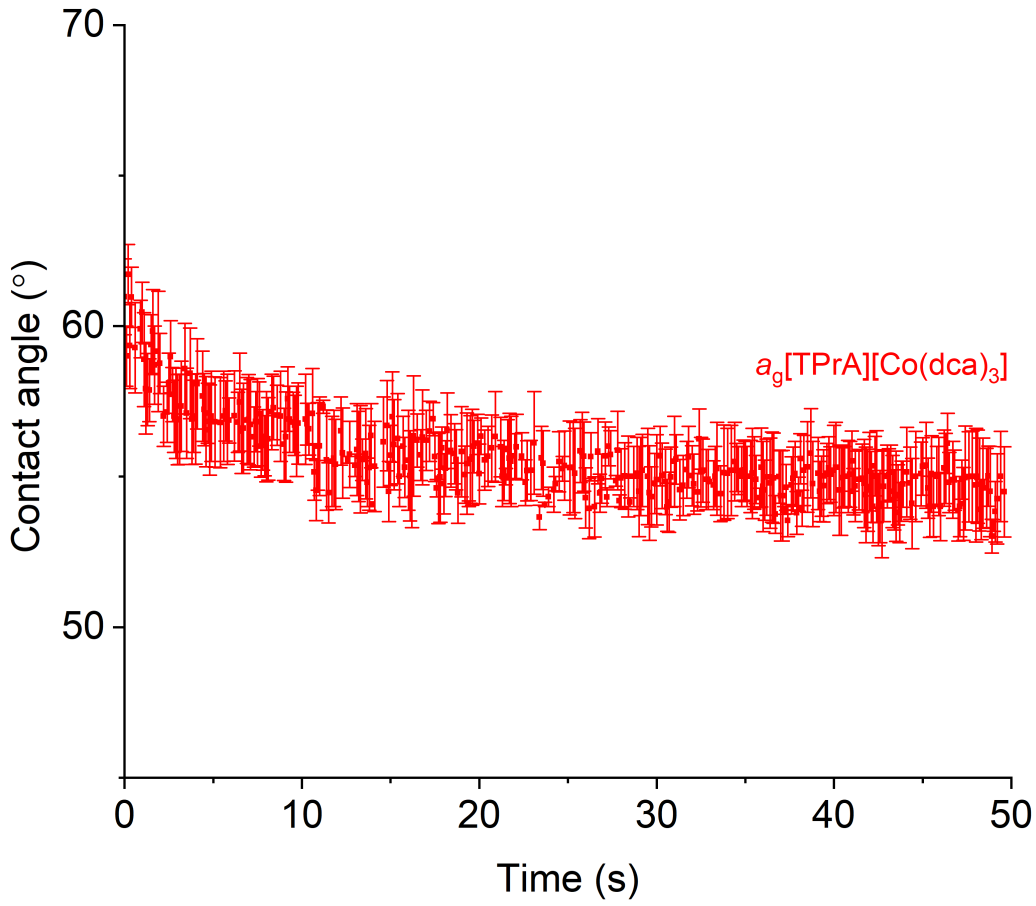

Figure S34. Water contact angle data collected on pelletised a_g[TPrA][Co(dca)$_3$] collected over 50 s. Anomalous data points have been excluded for clarity.

References:

[1] A. Coelho, Topas Academia V6., Coelho Software: Brisbane, Australia, 2007.
[2] TA Instruments Univeral Analysis, TA Instruments: New Castle, Delaware, USA, 2000.
[3] Netzsch Proteus, NETZSCH-Geratebau GmbH: Selb, Germany, 2021.
[4] MicroActive Version 4.04, Micromeritics Instrument Incorporation, 2017.
[5] R. Woodward, 2015.
[6] J. M. Bermúdez-García, M. Sánchez-Andújar, S. Yáñez-Vilar, S. Castro-García, R. Artiaga, J. López-Beceiro, L. Botana, A. Alegría and M. A. Señarís-Rodríguez, *J. Mater. Chem. C*, 2016, **4**, 4889–4898.
[7] J. M. Bermúdez-García, M. Sánchez-Andújar, S. Yáñez-Vilar, S. Castro-García, R. Artiaga, J. López-Beceiro, L. Botana, Á. Alegría and M. A. Señarís-Rodríguez, *Inorg. Chem.*, 2015, **54**, 11680–11687.
[8] B. K. Shaw, A. R. Hughes, M. Ducamp, S. Moss, A. Debnath, A. F. Sapnik, M. F. Thorne, L. N. McHugh, A. Pugliese, D. S. Keeble, P. Chater, J. M. Bermudez-Garcia, X. Moya, S. K. Saha, D. A. Keen, F. X. Coudert, F. Blanc and T. D. Bennett, *Nat. Chem.*, 2021, **13**, 778–785.